Available online at www.sciencedirect.com
SCIENCE DIRECT®
Coordination Chemistry Reviews 250 (2006) 1351–1372
COORDINATION CHEMISTRY REVIEWS
www.elsevier.com/locate/ccr

Review

Mononuclear metallacarboranes of groups 6–10 metals: Analogues of metallocenes Electrochemical and X-ray structural aspects

Maddalena Corsini, Fabrizia Fabrizi de Biani, Piero Zanello *

Dipartimento di Chimica dell'Università di Siena, Via Aldo Moro, 53100 Siena, Italy

Received 18 July 2005; accepted 8 December 2005
Available online 26 January 2006

Contents

* Corresponding author. Tel.: +39 057723 4262; fax: +39 057723 4254.
E-mail address: zanello@unisi.it (P. Zanello).

doi:10.1016/j.ccr.2005.12.009

Abstract

Metallacarboranes containing carborane ligands possessing a pentagonal open face can coordinate metal atoms in a η^5-manner quite similar to the cyclopentadienyl monoanion, thus affording metallocene analogues. By virtue of such an analogy, their electron transfer aptitude plays an important role in their physico-chemical characterisation. We review such an aspect, also providing evidence for the structural consequences of their electron transfer processes.

At variance with metallocenes, electrochemical investigations on the metallacarboranes have not yet become a routine tool to search for their potential application in fields which require electronic mobility.

Keywords: Metallacarboranes; Metallocenes; Electrochemistry; X-ray

1. Introduction

The chemistry of metallacarboranes was initiated by M.F. Hawthorne and his students in 1965 in an attempt to join the chemistry of polyhedral boranes to the emerging organometallic chemistry [1]. Inorganic chemists immediately realized that these derivatives opened a new direction in the development of organometallic and coordination chemistry, just as the chemistry

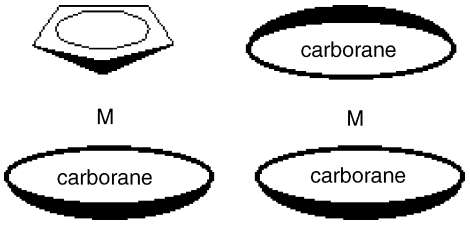

Chart 1. Metallacarborane sandwich analogues of metallocenes.

of metallocenes was having a major impact on many areas of chemistry. Since that time, many advances have been recorded in the theoretical and applicative aspects of the metallacarboranes, including the understanding of their striking analogy with metallocenes [2] or their potential use in medicinal chemistry [2a,f,3]. Obviously, the ability of carborane (or carbaborane) ligands to give rise to stable sandwich metal complexes draws attention toward one of the most important characteristics of metallocenes, namely their electrochemical behavior [4].

Accordingly, in the context of reporting our recent contribution to the redox chemistry of metallacarboranes, we update Geiger's electrochemical survey on metallacarboranes [4c], limited however to the half-sandwich and full-sandwich derivatives which can qualitatively mimic mononuclear metallocenes, Chart 1, and primarily to those that have been crystallographically characterized.

Therefore, we focus on metallacarboranes of groups 6–10 metals containing carborane ligands possessing a pentagonal, usually planar, open face that can form sandwich complexes with metal atoms via η^5-coordination in a manner directly analogous to the cyclopentadienyl monoanion. It is, however, noted that there are many examples of (X-ray authenticated) metallacarboranes in which the carborane ligands display hapticities other than 5 towards central metal ions [5–28].

Since we wish to give evidence for the structural consequences of electron transfer processes, we will report selected X-ray bond lengths (approximated to the nearest 0.01 Å, neglecting any ESD values) only in the cases of redox couples.

Finally, in order to simplify the numbering of metallocarborane cage vertices [29–31] and since we are limited to carborane ligands having coordinating pentagonal faces, we will adopt the simple numbering system shown in Fig. 1.

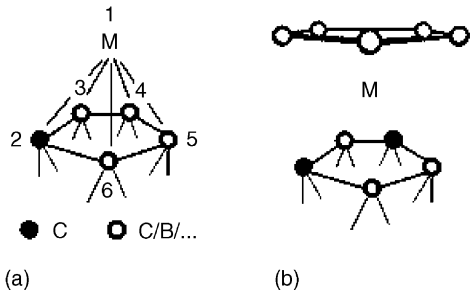

Fig. 1. (a) Numbering of the atoms present in the coordinating pentagonal faces of carborane ligands in metallocene-like metallacarboranes. (b) Example of the adopted numbering: [(η-C_5R_5) M(2,4-$C_2B_{3+x}H_y$)].

In cases where the carborane cage includes additional carbon atoms in lower polygons, we will continue clockwise giving priority to the carbon atom(s). We are confident that the draft of the different molecular structures will avoid any misunderstanding with respect to the canonical conventions, but the reader is recommended to make reference to the original papers.

2. CB_7 cages

2.1. Group 9 metallacarboranes

2.1.1. Cobaltacarboranes

2.1.1.1. Half-sandwich complexes. As far as we know, the only example of a crystallographically characterized half-sandwich CB_7 metallacarborane is [(η-C_5H_5)Co^{III}(CB_7H_8)]$^-$, in which the coordinated open face contains five boron atoms; in fact, the carbon atom occupies the opposed apical position [32]. Its electrochemical behavior has been reviewed [4c].

3. CB_8 cages

3.1. Group 9 metallacarboranes

3.1.1. Cobaltacarboranes

3.1.1.1. Half-sandwich complexes. The crystal structure of [(η-C_5H_5)Co(CB_8H_9)] is available [33].

4. CB_{10} cages

4.1. Group 8 metallacarboranes

4.1.1. Ferracarboranes

4.1.1.1. Half-sandwich complexes. The crystal structure of [(η-C_5H_5)Fe^{III}(2-OEt_2-2-$CB_{10}H_{10}$)] has been solved [34].

4.2. Group 9 metallacarboranes

4.2.1. Cobaltacarboranes

4.2.1.1. Half-sandwich complexes. Fig. 2 depicts the crystal structure of [(η-C_5H_5)Co(2-$CB_{10}H_{11}$)]$^-$ [35].[1]

In MeCN solution, it only exhibits an irreversible Co(III)/Co(IV) oxidation (E_p = +1.07 V, versus SCE) [36].

4.2.1.2. Full-sandwich complexes. The electrochemical behavior of [Co^{III}(2-$CB_{10}H_{11}$)$_2$]$^{3-}$ has been reported [4c].

4.3. Group 10 metallacarboranes

4.3.1. Nickelacarboranes

4.3.1.1. Half-sandwich complexes. [(η-C_5H_5)Ni(2-$CB_{10}H_{11}$)] exhibits in MeCN solution the sequential Ni(IV)/Ni(III)

[1] As a pictorial simplification, from hereafter carboranyl carbon and boron atoms will be simply represented as black and white balls, respectively.

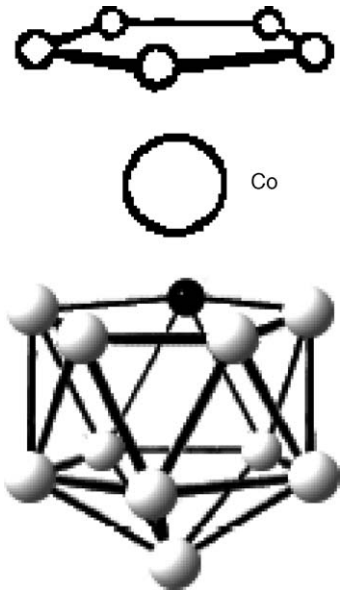

Fig. 2. The molecular structure of $[(\eta\text{-}C_5H_5)Co(2\text{-}CB_{10}H_{11})]^-$ (adapted from Ref. [35]).

($E^{\circ\prime} = -0.27$ V, versus SCE) and Ni(III)/Ni(II) ($E^{\circ\prime} = -1.57$ V) reduction processes [36].

The carbon-substituted $[(\eta\text{-}C_5H_5)Ni\{2\text{-}CH(SiMe_3)_2\text{-}2\text{-}CB_{10}H_{10})\}]$ [37] as well as its isomer having the carbon atom in the non-coordinating face [38] have been X-ray characterized.

5. C_2B_3 cages

The planar fragments $[C_2B_3H_5]^{2-}$ and $[C_2B_3H_3]^{4-}$ and their C-alkylated analogues, Scheme 1, which are known only as metal complexes and do not exist as free ions in solution, are isoelectronic with the cyclopentadienyl anion $[C_5H_5]^-$ and as such they can form metallocene-like complexes.

5.1. Group 9 metallacarboranes

5.1.1. Cobaltacarboranes

5.1.1.1. Half-sandwich complexes. The half-sandwich carboranes $[(\eta\text{-}C_5Me_5)Co\{\eta^5\text{-}2,3\text{-}Me_2\text{-}2,3\text{-}C_2B_3Me_3(\mu\text{-}H)_2\}]$ [39], $[(\eta\text{-}C_5Me_5)Co\{\eta^5\text{-}2,3\text{-}Et_2\text{-}2,3\text{-}C_2B_3H_4\text{-}5\text{-}C(=CH_2)OC(O)Me\}]$ [40] have been crystallographically characterized, but no pertinent electrochemical data are available.

The only electrochemical information is concerned with complexes $[(\eta\text{-}C_5Me_5)Co^{III}(\eta^5\text{-}2,3\text{-}Et_2\text{-}2,3\text{-}C_2B_3H_5)]$ and $[(\eta\text{-}C_5Me_5)Co^{III}(\eta^5\text{-}2,3\text{-}Et_2\text{-}C_2B_3H_4\text{-}5\text{-}Cl)]$ shown in Scheme 2.

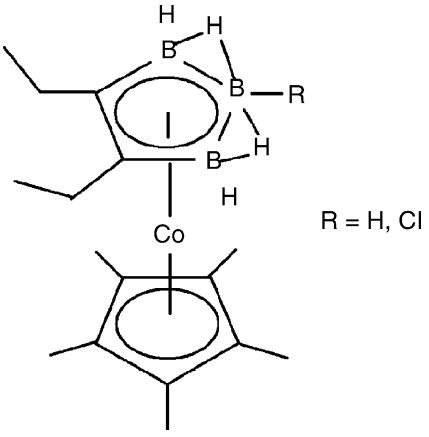

Scheme 2. Structure of $[(C_5Me_5)Co^{III}(\eta^5\text{-}2,3\text{-}Et_2\text{-}C_2B_3H_{5-x}\text{-}5\text{-}Cl_x)]$ ($x = 0, 1$).

In CH_2Cl_2 solution both the derivatives undergo an irreversible one-electron oxidation $\{[(C_5Me_5)Co(Et_2C_2B_3H_5)]$: $E_p = +0.98$ V, versus SCE; $[(C_5Me_5)Co(Et_2C_2B_3H_4Cl)]$: $E_p = +0.91$ V, versus $Fc^+/Fc\}$ [41,42], which testifies to the extreme lability of the Co(IV) oxidation state under the actual assembly. In dimethoxyethane (DME) solution, the chloro-substituted complex also undergoes irreversibly the sequence Co(III)/Co(II)/Co(I) at notably negative potential values ($E_p = -2.70$ and -2.97 V, versus Fc^+/Fc, respectively [42]).

6. C_2B_4 cages

The pentagonal pyramidal dianion $[R_2C_2B_4H_4]^{2-}$, in both the isomeric forms illustrated in Scheme 3, is isoelectronic with the cyclopentadienyl anion $[C_5H_5]^-$ and like this latter forms pentahapto metal complexes.

In reality, the fact that $[R_2C_2B_4H_4]^{2-}$ bears an excess of negative charge with respect to $[C_5R_5]^-$ can trigger significant different physico-chemical properties. Therefore, "charge-compensated" dicarbollide ligands have been prepared inserting two-electron donor substituents on the B atoms of the C_2B_3 face [2n] (a synthetic pattern mostly used in the case of $[C_2B_9H_{11}]^{2-}$, Section 8).

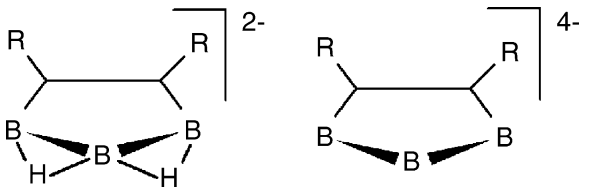

Scheme 1. The planar geometry of the anions $[R_2C_2B_3H_5]^{2-}$ and $[R_2C_2B_3H_3]^{4-}$.

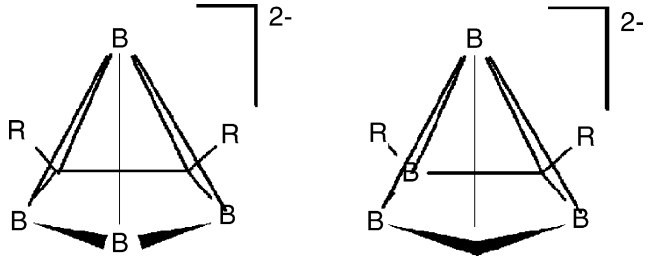

Scheme 3. Pyramidal geometry of the "carbon adjacent" and "carbon apart" isomers of the dianion $[R_2C_2B_4H_4]^{2-}$.

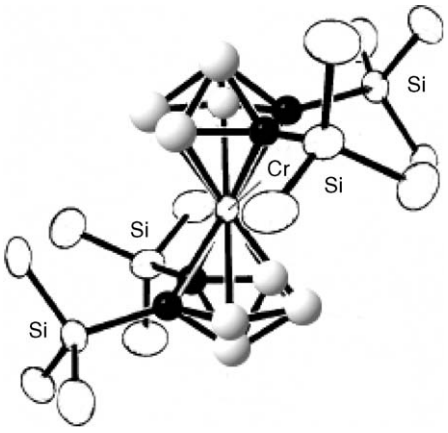

Fig. 3. The molecular structure of $[Cr^{III}\{2,3\text{-}(SiMe_3)_2\text{-}2,3\text{-}C_2B_4H_4\}_2]^-$ (adapted from Ref. [43]).

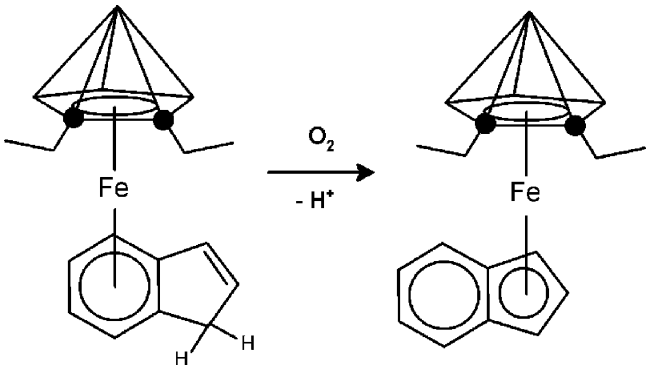

Scheme 4. Conversion of $[(\eta^6\text{-}C_9H_8)Fe^{II}(2,3\text{-}Et_2\text{-}2,3\text{-}C_2B_4H_4)]$ to $[(\eta^5\text{-}C_9H_8)Fe^{III}(2,3\text{-}Et_2\text{-}2,3\text{-}C_2B_4H_4)]$.

6.1. Group 6 metallacarboranes

6.1.1. Chromacarboranes

6.1.1.1. Full-sandwich complexes. Fig. 3 shows the molecular structure of the monoanion $[Cr^{III}\{2,3\text{-}(SiMe_3)_2\text{-}2,3\text{-}C_2B_4H_4\}_2]^-$ [43].

Although no electrochemical investigation has been carried out, chemical oxidation of the monoanion afforded the neutral complex $[Cr^{IV}\{2,3\text{-}(SiMe_3)_2\text{-}2,3\text{-}C_2B_4H_4\}_2]^0$, which substantially maintains the molecular structure of the monoanion precursor, but with some slight elongation of the Cr-ligand bond lengths, Table 1 [43,44].

The elongation of the bonding distances on passing from Cr(III) to Cr(IV) is shorter than that observed in the Cr(II)/Cr(III) couple $[Cr(C_5Me_5)_2]^{0/+}$ [45].

The monosubstituted complex $[Cr^{III}\{2\text{-}(SiMe_3)_2\text{-}2,3\text{-}C_2B_4H_5\}_2]^-$ has been also structurally characterized [43].

6.2. Group 8 metallacarboranes

6.2.1. Ferracarboranes

6.2.1.1. Half-sandwich complexes. $[(\eta\text{-}C_5H_5)Fe^{III}(2,3\text{-}C_2B_4H_6)]$ undergoes in MeCN solution the reversible Fe(III)/Fe(II) reduction ($E^{\circ\prime} = -0.52$ V). An irreversible oxidation (likely attributable to the Fe(III)/Fe(IV) process) is also detectable [46].

The crystallographically characterized indenylferracarborane $[(\eta^6\text{-}C_9H_8)Fe^{II}(2,3\text{-}Et_2\text{-}2,3\text{-}C_2B_4H_4)]$ upon deprotonation converts to $[(\eta^5\text{-}C_9H_8)Fe^{III}(2,3\text{-}Et_2\text{-}2,3\text{-}C_2B_4H_4)]$, Scheme 4 [47].

The Fe(III) complex exhibits the (partially chemically) reversible cathodic reduction to the corresponding Fe(II) derivative (in CH_2Cl_2: $E^{\circ\prime} = -0.64$ V; in DME: $E^{\circ\prime} = -0.70$ V; V, versus SCE) [47].

A similar electrochemical behavior is exhibited by $[(\eta\text{-}C_5Me_5)Fe^{III}(2,3\text{-}Et_2\text{-}2,3\text{-}C_2B_4H_4)]$ (obtained by deprotonation of $[(\eta\text{-}C_5Me_5)Fe^{II}H(2,3\text{-}Et_2\text{-}2,3\text{-}C_2B_4H_4)]$) [48]. In fact, it also undergoes reversibly the reduction to the corresponding Fe(II) species (in DME: $E^{\circ\prime} = -0.88$ V; in MeCN: $E^{\circ\prime} = -0.91$ V; in CH_2Cl_2: $E^{\circ\prime} = -0.96$ V; V, versus SCE) [48].

6.2.1.2. Full-sandwich complexes. Complexes $[(2,3\text{-}Me_2\text{-}2,3\text{-}C_2B_4H_4)_2FeH_2]$ [49] and $[\{2,4\text{-}(SiMe_3)_2\text{-}2,4\text{-}C_2B_4H_4\}_2FeH]$ [50a] have been structurally characterized.

6.2.2. Ruthenacarboranes

6.2.2.1. Half-sandwich complexes. The crystal structure of $[(\eta\text{-}C_5Me_5)Ru^{II}H(2,3\text{-}Et_2\text{-}2,3\text{-}C_2B_4H_4)]$ is known [51].

6.3. Group 9 metallacarboranes

6.3.1. Cobaltacarboranes

6.3.1.1. Half-sandwich complexes. The electrochemical behavior of the crystallographically characterized $[(\eta\text{-}C_5H_5)Co^{III}(2,3\text{-}Me_2\text{-}2,3\text{-}C_2B_4H_4)]$ [52] and that of the unsubstituted $[(\eta\text{-}C_5H_5)Co^{III}(2,3\text{-}C_2B_4H_6)]$ and $[(\eta\text{-}C_5H_5)Co^{III}(2,4\text{-}C_2B_4H_6)]$ have been reviewed [4c].

One of the most useful precursors in C_2B_4 cobaltacarboranes is $[(\eta\text{-}C_5Me_5)Co^{III}(2,3\text{-}Et_2\text{-}2,3\text{-}C_2B_4H_4)]$, the crystal structure of which has not been yet resolved (but the crystal structure of $[(\eta\text{-}C_5Me_5)Co^{II}(2,3\text{-}Et_2\text{-}2,3\text{-}C_2B_4H_3\text{-}6\text{-}I)]^-$ [53] is available). It undergoes both Co(III)/Co(IV) oxidation (which is reversible in CH_2Cl_2 solution) and Co(III)/Co(II) reduction (which is reversible in DME solution) [54].

The pertinent electrode potentials are compiled in Table 2, together with those of a few related species.

The crystal structures of the half-sandwich complexes with the carborane ligand fused to lateral rings $[(\eta\text{-}C_5H_5)Co\{2,3\text{-}$

Table 1
Selected bonding distances (Å) in the Cr(III)/Cr(IV) couple $[Cr\{2,3\text{-}(SiMe_3)_2\text{-}2,3\text{-}C_2B_4H_4\}_2]^{-/0}$

Complex	Cr-centroid	Cr-C2	Cr-C3	Cr-B4	Cr-B5	Cr-B6
$[Cr^{III}\{2,3\text{-}(SiMe_3)_2\text{-}2,3\text{-}C_2B_4H_4\}_2]^-$	1.78	2.16	2.15	2.22	2.32	2.26
$[Cr^{IV}\{2,3\text{-}(SiMe_3)_2\text{-}2,3\text{-}C_2B_4H_4\}_2]^0$	1.81	2.19	2.17	2.30	2.38	2.28

Table 2
Formal electrode potentials (V, vs. SCE) for the redox changes exhibited by $[(C_5Me_5)Co^{III}(Et_2C_2B_4H_4)]$ and related species

Complex	$E^\circ_{Co(IV)/Co(III)}$	$E^\circ_{Co(III)/Co(II)}$	Solvent	Reference
$[(\eta\text{-}C_5Me_5)Co^{III}(2,3\text{-}Et_2\text{-}2,3\text{-}C_2B_4H_4)]$	+1.43[a]	−1.99	DME	[54]
	+1.27	–	CH_2Cl_2	[54]
	–	−1.73	THF	[55]
	+1.41	–	CH_2Cl_2	[55]
	+1.16	–	CH_2Cl_2	[41]
$[(\eta\text{-}C_5Me_5)Co^{III}(2,3\text{-}Me_2\text{-}2,3\text{-}C_2B_4H_4)]$	–	−1.92	DME	[54]
$[(\eta\text{-}C_5Me_5)Co^{III}\{2,3\text{-}(SiMe_3)_2\text{-}2,3\text{-}C_2B_4H_4\}]$	–	−1.77	DME	[54]
$[(\eta\text{-}C_5H_5)Co^{III}(2,3\text{-}Me_2\text{-}2,3\text{-}C_2B_4H_4)]$	+1.14[a]	−1.69	MeCN	[46,4c]

[a] Peak-potential value for irreversible process.

$(SiMe_3)_2$-2,3-$C_2B_4H_3$-$B_2H_5\}$] [56] and $[(\eta\text{-}C_5H_5)Co\{2,3\text{-}Me_2\text{-}2,3\text{-}C_2B_4H_3\}\text{-}\{2',3'\text{-}Me_2\text{-}2,3\text{-}C_2B_4H_5\}]$ [57] are known.

6.3.1.2. Full-sandwich complexes. The crystal structures of the full-sandwich monoanions $[Co(2,3\text{-}Et_2\text{-}2,3\text{-}C_2B_4H_4)_2]^-$ [58], $[Co\{2,3\text{-}(SiMe_3)_2\text{-}2,3\text{-}C_2B_4H_4\}_2]^-$ [50a,59], and the mixed-ligand $[\{\eta^5\text{-}2,3\text{-}Me_2\text{-}2,3\text{-}C_2B_4H_3\}Co\{\eta^5\text{-}2,3\text{-}Me_2\text{-}2,3\text{-}C_2B_3H_5\}]^-$ [60] are available.

6.3.2. Iridacarboranes

6.3.2.1. Half-sandwich complexes. The crystal structure of $[(\eta\text{-}C_5Me_5)Ir(2,3\text{-}Et_2\text{-}2,3\text{-}C_2B_4H_4)]$ is known [61].

6.4. Group 10 metallacarboranes

6.4.1. Nickelacarboranes

6.4.1.1. Full-sandwich complexes. The solid-state molecular structure of $[Ni^{IV}\{2,4\text{-}(SiMe_3)_2\text{-}2,4\text{-}C_2B_4H_4\}_2]$ is shown in Fig. 4 [50b].

In CH_2Cl_2 solution it undergoes a one-electron reduction, but the relative potential value has not been reported [50a].

The crystal structure of the "charge compensated" $[\{2,4\text{-}(SiMe_3)_2\text{-}5,6\text{-}(N(Me)(CH_2)_2N(Me)_2)\text{-}2,4\text{-}C_2B_2H_2\}Ni\{2',4'\text{-}(SiMe_3)_2\text{-}2',4'\text{-}C_2B_4H_4\}]$ is available [50a].

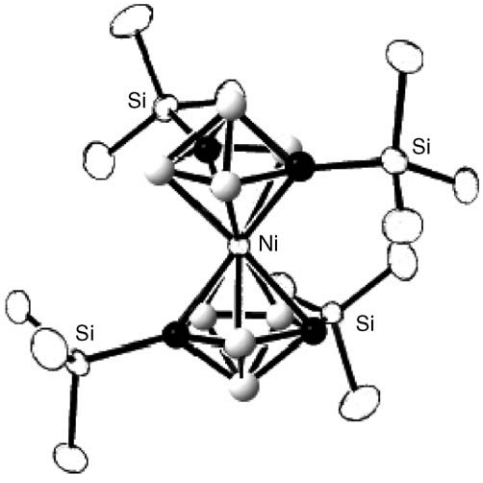

Fig. 4. The molecular structure of $[Ni\{2,4\text{-}(SiMe_3)_2\text{-}2,4\text{-}C_2B_4H_4\}_2]$ (adapted from Ref. [50b]).

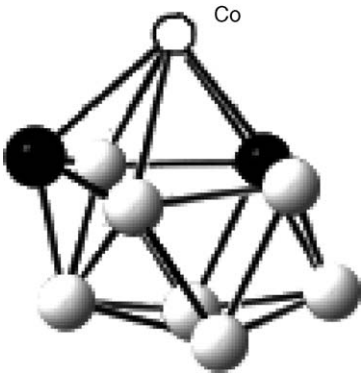

Fig. 5. The molecular structure of $[(\eta\text{-}C_5H_5)Co(2,4\text{-}C_2B_7H_9)]$ (adapted from Ref. [62b]).

7. C_2B_7 cages

7.1. Group 9 metallacarboranes

7.1.1. Cobaltacarboranes

7.1.1.1. Half-sandwich complexes. The crystal structure of $[(\eta\text{-}C_5H_5)Co^{III}(2,4\text{-}C_2B_7H_9)]$ [62a,b] is available. The non-planarity of the η^5-B_3C_2 face of the dianion $[C_2B_7H_9]^{2-}$ is shown in Fig. 5.

The electrochemical behavior of different isomers of $[(\eta\text{-}C_5H_5)Co(C_2B_7H_9)]$ has been reviewed [4c].

7.1.1.2. Full-sandwich complexes. The X-ray structure of $[Co^{III}(2,4\text{-}C_2B_7H_9)_2]^-$ has been solved [63].

8. C_2B_9 cages

The isomeric dicarbollide dianions $[C_2B_9H_{11}]^{2-}$ (carbon atoms adjacent or apart), Scheme 5, which are the most diffuse ligands in metallacarboranes, have a 12-vertex icosahedral geometry in which the coordinating pentagonal C_2B_3 face is planar and pioneeringly recognized as isoelectronic with the cyclopentadienyl anion [64].

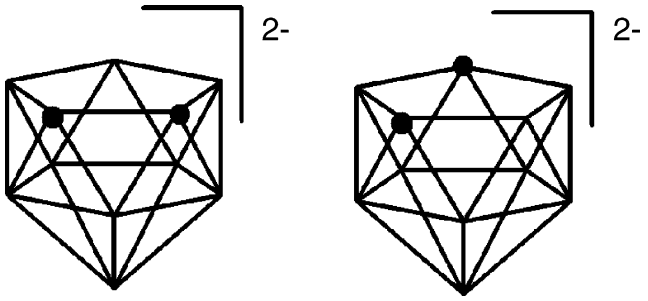

Scheme 5. Structure of two isomeric forms of the dianion $[C_2B_9H_{11}]^{2-}$.

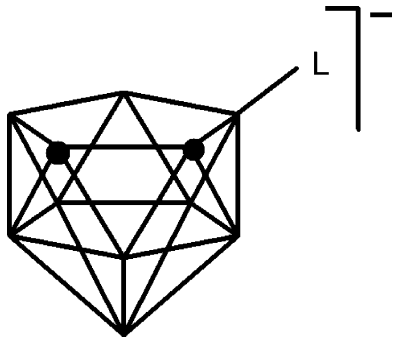

Scheme 6. The monoanion $[LC_2B_9H_{10}]^-$ is a representative example of charge-compensated dicarbollide ligands.

Nevertheless, as previously mentioned in Section 6, since $[C_2B_9H_{11}]^{2-}$ bears an excess of negative charge with respect to $[C_5R_5]^-$ (thus potentially triggering significant different physico-chemical properties), "charge-compensated" dicarbollide ligands have been prepared [65]. For instance, the monoanion $[LC_2B_9H_{10}]^-$, Scheme 6, has been obtained by inserting a two-electron donor substituent on one of the three B atoms of the C_2B_3 face.

A further architecture of the metalla-C_2B_9 assembly is that we will define as "metallacarboranophanes", Scheme 7, in which, as happens in "ferrocenophanes" [45], there are carbon or heteroatomic chains which bridge the two half-sandwich carborane ligands.

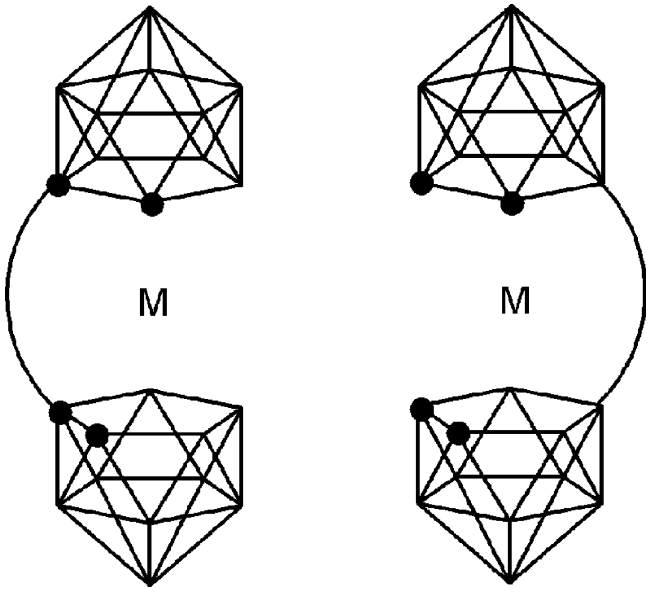

Scheme 7. Typical metallacarboranes having B/B or C/C bridging chains.

8.1. Group 6 metallacarboranes

8.1.1. Chromacarboranes

8.1.1.1. Full-sandwich complexes. The crystal structures of both $[Cr^{III}(2,3\text{-}C_2B_9H_{11})_2]^-$ [66] and that of the methyl-substituted monoanion $[Cr^{III}(2,3\text{-}Me_2\text{-}2,3\text{-}C_2B_9H_9)_2]^-$ have been solved [67]. The electrochemistry of $[Cr^{III}(2,3\text{-}C_2B_9H_{11})_2]^-$ showed no reversible redox processes [4c].

8.2. Group 8 metallacarboranes

8.2.1. Ferracarboranes

8.2.1.1. Classical (charge-noncompensated) complexes.

8.2.1.1.1. Half-sandwich complexes. Fig. 6 shows the classical sandwich geometry of the X-ray characterized $[(\eta\text{-}C_5H_5)Fe^{III}(2,3\text{-}C_2B_9H_{11})]$ [68,69]. It exhibits the reversible reduction to the corresponding Fe(II) monoanion [4a,69]. The redox potentials in different solvents are compiled in Table 3.

The crystal structure of $[(\eta\text{-}C_5H_5)Fe^{II}(2,3\text{-}C_2B_9H_{11})]^-$ has been solved [69]. The most significant structural changes accompanying the Fe(III)/Fe(II) reduction are compiled in Table 4.

The general elongation of the bond distances following the passage from Fe(II) to Fe(III) is reminiscent the ferrocene/ferrocenium transition [45]. The crystal structures of $[(\eta\text{-}C_5H_5)Fe\{5\text{-}OC(O)CF_3\text{-}2,3\text{-}C_2B_9H_{10}\}]$ [70], $[(\eta\text{-}C_5H_5)Fe\{3\text{-}CH(OEt)_2\text{-}2,3\text{-}C_2B_9H_{10}\}]$ [71] and $[(\eta^5\text{-}C_9H_7)Fe(2,3\text{-}C_2B_9H_{11})]$ [72] are available.

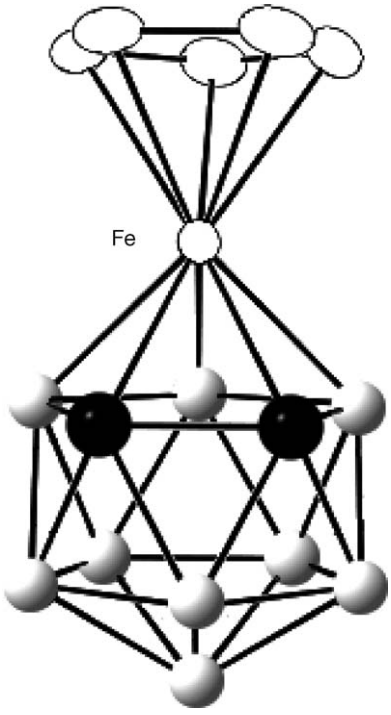

Fig. 6. The molecular structure of $[(\eta\text{-}C_5H_5)Fe^{III}(2,3\text{-}C_2B_9H_{11})]$ (adapted from Ref. [69]).

Table 3
Formal electrode potentials (V, vs. SCE) for the Fe(II)/Fe(III) passage in different solvents for the process $[(\eta\text{-}C_5H_5)Fe(2,3\text{-}C_2B_9H_{11})]^{0/-}$

$E^{\circ\prime}_{Fe(III)/Fe(II)}$	Solvent	Reference
−0.08	MeCN	[4a]
−0.03	MeCN	[69]
−0.04	THF	[69]
−0.18	CH_2Cl_2	[69]

8.2.1.1.2. Full-sandwich complexes. The crystal structure of $[Fe^{II}(2,3\text{-}C_2B_9H_{11})_2]^{2-}$ has been reported [73]. Like the related half-sandwich complex, it exhibits the reversible Fe(II)/Fe(III) passage [4c]. In fact, the monoanion $[Fe^{III}(2,3\text{-}C_2B_9H_{11})_2]^{-}$ has been X-ray characterized [66a,74]. Pertinent bond lengths for the redox couple $[Fe(2,3\text{-}C_2B_9H_{11})_2]^{-/2-}$ are compiled in Table 5.

Also in this case, the Fe(II)/Fe(III) passage involves elongation of the Fe-ligand distances.

The crystal structure of the C/C-thiophene substituted $[Fe^{III}(2\text{-}C_4H_3S\text{-}2,3\text{-}C_2B_9H_{10})_2]^{-}$ is available [66b,75]. It undergoes the Fe(III)/Fe(II) reduction at a potential value slightly less negative than that of the unsubstituted $[Fe^{III}(2,3\text{-}C_2B_9H_{11})_2]^{-}$ ($E^{\circ\prime} = -0.34$ V, versus SCE, in MeCN solution [75] versus −0.42 V, versus SCE, in Me_2CO/H_2O (1:1) solution) [4c].

8.2.1.2. Charge-compensated complexes.

8.2.1.2.1. Half-sandwich complexes. A series of half-sandwich charge-compensated complexes have been characterized. As a typical example, Fig. 7 shows the crystal structure of the half-sandwich $[(\eta\text{-}C_5Me_5)Fe^{III}(6\text{-}Me_2S\text{-}2,3\text{-}C_2B_9H_{10})]^{+}$ [76].

The crystal structures of $[(\eta\text{-}C_5Me_5)Fe^{II}(6\text{-}Me_3N\text{-}2,3\text{-}C_2B_9H_{10})]$ [69] and $(\eta\text{-}C_5H_5)Fe^{II}(4,5\text{-}Br_2\text{-}6\text{-}Me_2S\text{-}2,3\text{-}C_2B_9H_8)]$ [77] have been also resolved. The Fe(II) complexes undergo reversibly the Fe(II)/Fe(III) oxidation at potential values notably higher that the classical analog [69]. The pertinent formal electrode potentials are compiled in Table 6. Minor variations in oxidation potentials are obviously due to the different inductive effects of the charge-compensating groups.

8.2.1.2.2. Full-sandwich complexes. Fig. 8 shows the molecular structure of the full-sandwich DD/LL racemate

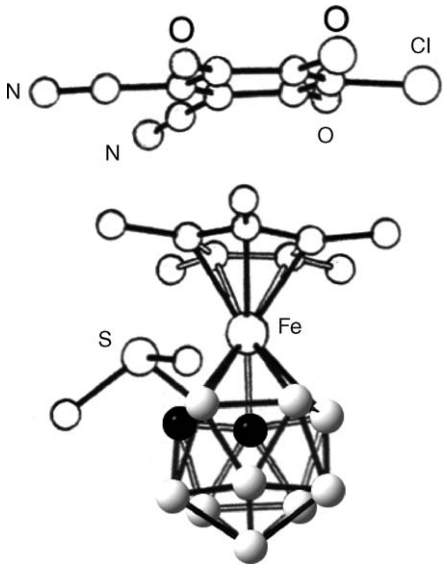

Fig. 7. The molecular structure of $[(\eta\text{-}C_5Me_5)Fe^{III}(6\text{-}Me_2S\text{-}2,3\text{-}C_2B_9H_{10})][ddq]$ (ddq = 2,3-dichloro-5,6-dicyano-*p*-benzoquinone) (adapted from Ref. [76]).

Table 6
Formal electrode potentials (V, vs. SCE) for the Fe(II)/Fe(III) passage in charge-compensated half-sandwich complexes

Complex	$E^{\circ\prime}$	Solvent	Reference
$[(\eta\text{-}C_5Me_5)Fe(6\text{-}Me_2S\text{-}2,3\text{-}C_2B_9H_{10})]^{0/+}$	+0.18	MeCN	[76]
	+0.21	CH_2Cl_2	[69]
$[(\eta\text{-}C_5H_5)Fe(6\text{-}Me_2S\text{-}2,3\text{-}C_2B_9H_{10})]^{0/+}$	+0.47	CH_2Cl_2	[69]
$[(\eta\text{-}C_5H_5)Fe(6\text{-}Me_2S\text{-}2,3\text{-}Me_2C_2B_9H_8)]^{0/+}$	+0.49	CH_2Cl_2	[69]
$[(\eta\text{-}C_5H_5)Fe(6\text{-}Me_3N\text{-}2,3\text{-}C_2B_9H_{10})]^{0/+}$	+0.40	CH_2Cl_2	[69]
$[(\eta\text{-}C_5H_5)Fe(6\text{-}C_5H_5N\text{-}2,3\text{-}C_2B_9H_{10})]^{0/+}$	+0.40	CH_2Cl_2	[69]

$[Fe^{II}(6\text{-}Me_2S\text{-}2,3\text{-}C_2B_9H_{11})_2]$ [78] in which the C_2B_3 coordinating faces are staggered and assume a cisoid arrangement (a quite similar structure is exhibited by the *meso* form [79]). In nonaqueous solvents it exhibits the reversible Fe(II)/Fe(III) oxidation (MeCN: $E^{\circ\prime} = +0.45$ V [78]; CH_2Cl_2: $E^{\circ\prime} = +0.55$ V [69]; V, versus SCE), which, because of both electrostatic and inductive effects, occurs at more positive potential values than the classical $[Fe(2,3\text{-}C_2B_9H_{11})_2]^{2-}$. In fact, the monocation $[Fe^{III}(6\text{-}Me_2S\text{-}2,3\text{-}C_2B_9H_{10})_2]^{+}$ has been crystallographically

Table 4
Selected metal-bond (average) distances (Å) in the Fe(III)/Fe(II) couple $[(\eta\text{-}C_5H_5)Fe(2,3\text{-}C_2B_9H_{11})]^{0/-}$ [69]

Complex	Fe-C_2B_3 centroid	Fe-C_5H_5 centroid	Fe-C2	Fe-C3	Fe-B4	Fe-B5	Fe-B6
$[(C_5H_5)Fe^{III}(2,3\text{-}C_2B_9H_{11})]$	1.49	1.72	2.07	2.07	2.09	2.10	2.10
$[(C_5H_5)Fe^{II}(2,3\text{-}C_2B_9H_{11})]^{-}$	1.44	1.66	2.01	2.01	2.07	2.08	2.11

Table 5
Selected metal-bond (average) distances (Å) in the Fe(II)/Fe(III) couple $[Fe(2,3\text{-}C_2B_9H_{11})_2]^{-/2-}$

Complex	Fe-C_2B_3 centroid	Fe-C2	Fe-C3	Fe-B4	Fe-B5	Fe-B6	Reference
$[Fe^{II}(2,3\text{-}C_2B_9H_{11})_2]^{2-}$	1.48	2.02	2.05	2.07	2.11	2.14	[73a]
$[Fe^{III}(2,3\text{-}C_2B_9H_{11})_2]^{-}$	1.53	2.09	2.09	2.13	2.14	2.13	[66a]

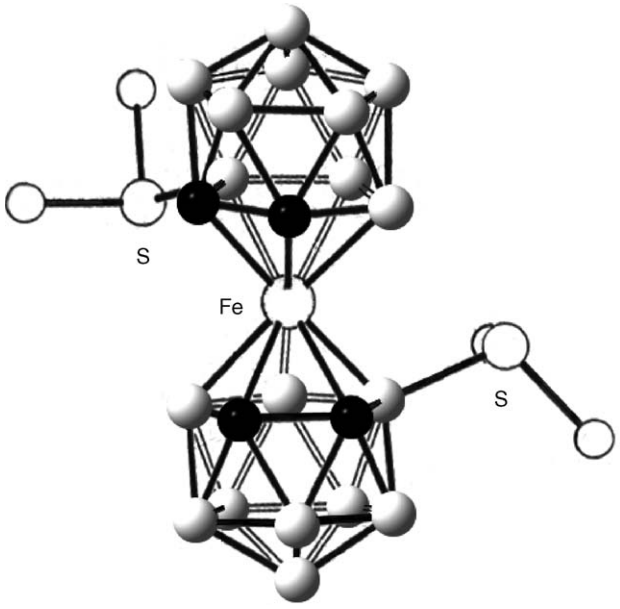

Fig. 8. The molecular structure of $[Fe^{II}(6\text{-}Me_2S\text{-}2,3\text{-}C_2B_9H_{10})_2]$ (adapted from Ref. [79]).

characterized [78]. It essentially maintains the molecular structure of its Fe(II) precursor. A few selected bond lengths are summarized in Table 7.

As expected, also in this case, the Fe(II)/Fe(III) passage involves elongation of the Fe-ligand distances. The crystal structure of the isomer $[Fe^{II}(5\text{-}Me_2S\text{-}2,3\text{-}C_2B_9H_{10})_2]^0$ [80] and that of $[Fe^{II}(5\text{-}NEt_3\text{-}2,3\text{-}C_2B_9H_{10})_2]$ [73] are also known. Comparison between the redox potentials of $[Fe(6\text{-}Me_2S\text{-}2,3\text{-}C_2B_9H_{10})_2]^{0/+}$ and $[(\eta\text{-}C_5H_5)Fe(6\text{-}Me_2S\text{-}2,3\text{-}C_2B_9H_{10})]^{0/+}$ suggests that the anion $[Me_2S\text{-}2,3\text{-}C_2B_9H_{10}]^-$ not only is isoelectronic with $[C_5H_5]^-$ but also plays the same overall inductive effects. The differences between the other redox couples are easily accounted for by simple electron-donating effects (C_5H_5 versus C_5Me_5) or coulombic effects due to the different overall charges.

8.2.1.2.3. Carboranophane complexes. Fig. 9 exemplifies the crystal structures of both a C/C bridged and a B/B bridged ferracarboranophane, respectively [81,82]. The Fe-C_2B_3 bond distances are substantially similar to those of $[Fe^{II}(2,3\text{-}C_2B_9H_{11})_2]^{2-}$. The electrochemical behavior of $[Fe^{III}(2,4\text{-}C_2B_9H_{10})_2\{\mu\text{-}C_3N_2H_3\}]$ in MeCN solution exhibits the reversible Fe(III)/Fe(II) reduction ($E^{\circ\prime} = +0.30$ V, versus SCE) [82], which, compared to the redox potential of the couple $[Fe(2,3\text{-}C_2B_9H_{11})_2]^{2-/-}$ ($E^{\circ\prime} = -0.42$ V, in aqueous Me_2CO solution), indicates that the bridging pyrazole ligand makes easier the electron addition. The crystal structure of the B/B bridged $[Fe^{III}(2,4\text{-}C_2B_9H_{10})_2\{\mu\text{-}OMe\}]$ is known [83].

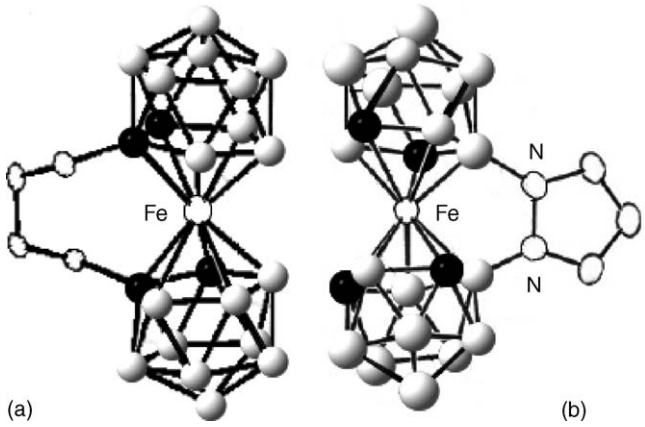

Fig. 9. The molecular structures of: (a) $[Fe^{III}(2,3\text{-}C_2B_9H_{10})_2\{\mu\text{-}C_4H_8\}]^-$ and (b) $[Fe^{III}(2,4\text{-}C_2B_9H_{10})_2\{\mu\text{-}C_3N_2H_3\}]$ (adapted from Refs. [81,82], respectively).

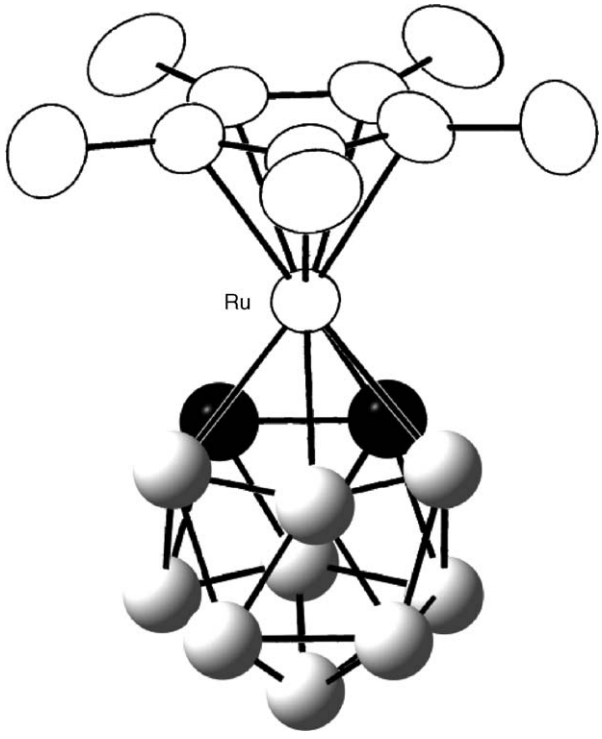

Fig. 10. The molecular structure of $[(\eta\text{-}C_5Me_5)Ru(2,3\text{-}C_2B_9H_{11})]^-$ (adapted from Ref. [84]).

8.2.2. Ruthenacarboranes

8.2.2.1. Classical (charge-noncompensated) complexes.

8.2.2.1.1. Half-sandwich complexes. Fig. 10 shows the solid state structure of $[(\eta\text{-}C_5Me_5)Ru(2,3\text{-}C_2B_9H_{11})]^-$ [84].

Table 7
Selected metal-bond (average) distances (Å) in the Fe(II)/Fe(III) couple $[Fe(6\text{-}Me_2S\text{-}2,3\text{-}C_2B_9H_{10})_2]^{0/+}$ [79]

Complex	Fe-C_2B_3 centroid	Fe-C2	Fe-C3	Fe-B4	Fe-B5	Fe-B6
$[Fe^{II}(6\text{-}Me_2S\text{-}2,3\text{-}C_2B_9H_{10})_2]^0$	1.50	2.04	2.04	2.09	2.15	2.11
$[Fe^{III}(6\text{-}Me_2S\text{-}2,3\text{-}C_2B_9H_{10})_2]^+$	1.54	2.08	2.09	2.13	2.13	2.28

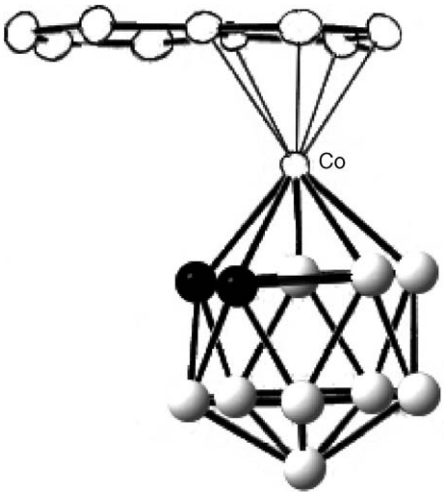

Fig. 11. The molecular structure of $[(\eta^5\text{-}C_9H_7)Co^{III}(2,3\text{-}C_2B_9H_{11})]$ (adapted from Ref. [88]).

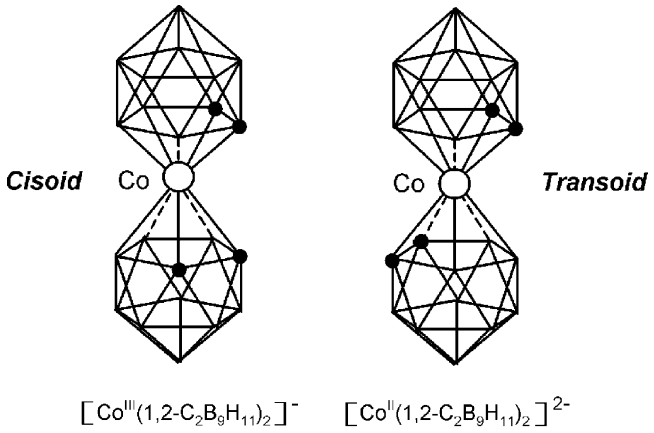

Scheme 8. Rotational geometries of the couple $[Co(2,3\text{-}C_2B_9H_{11})_2]^{-/2-}$.

In CH_2Cl_2 solution the Ru(II)/Ru(III) oxidation process is chemically reversible in the short times of cyclic voltammetry ($E^{\circ\prime} = +0.13$ V, versus SCE), but accompanied by slow degradation in the longer times of exhaustive electrolysis [85].

8.2.2.2. Charge-compensated complexes.

8.2.2.2.1. Half-sandwich complexes. The crystal structures of a series of charge compensated half-sandwich ruthenacarboranes (namely, $[(\eta\text{-}C_5Me_5)Ru(6\text{-}SMe_2\text{-}2,3\text{-}C_2B_9H_{10})]$, $[(\eta\text{-}C_5Me_5)Ru(2\text{-}Ph\text{-}5\text{-}SMe_2\text{-}2,3\text{-}C_2B_9H_9)]$, $[(\eta\text{-}C_5Me_5)Ru(3\text{-}Ph\text{-}4\text{-}SMe_2\text{-}2,3\text{-}C_2B_9H_9)]$ are available [86]. As happens for the Fe(II) analog, $[(\eta\text{-}C_5Me_5)Ru(6\text{-}SMe_2\text{-}2,3\text{-}C_2B_9H_{10})]$ undergoes in CH_2Cl_2 solution the Ru(II)/Ru(III) oxidation with features of partial chemical reversibility at potential values notably higher than $[(\eta\text{-}C_5Me_5)Ru(2,3\text{-}C_2B_9H_{11})]^-$ ($E^{\circ\prime} = +0.70$ V, versus +0.13 V) [85].

8.3. Group 9 metallacarboranes

8.3.1. Cobaltacarboranes

8.3.1.1. Classical (charge-noncompensated) complexes.

8.3.1.1.1. Half-sandwich complexes. The crystal structure of the half-sandwich complex $[(\eta\text{-}C_5H_5)Co^{III}(2,3\text{-}C_2B_9H_{11})]$ is known [88]. In nonaqueous solution it undergoes reversibly the sequence Co(III)/Co(II)/Co(I) (in MeCN: $E^{\circ\prime} = -1.21$ and -2.11 V, respectively [4c]; in THF: $E^{\circ\prime} = -1.18$ and -2.23 V, respectively [87]; V, versus SCE). The crystal structure of the methylated analogue $[(\eta\text{-}C_5Me_5)Co^{III}(2,3\text{-}C_2B_9H_{11})]$ is also known [13d]. The molecular structure of the indenylcobaltacarborane $[(\eta^5\text{-}C_9H_7)Co^{III}(2,3\text{-}C_2B_9H_{11})]$ is shown in Fig. 11 [88].

Like $[(\eta\text{-}C_5H_5)Co^{III}(2,3\text{-}C_2B_9H_{11})]$, it exhibits in CH_2Cl_2 solution the reversible sequence Co(III)/Co(II)/Co(I) at the $E^{\circ\prime}$ values -0.85 and -1.87 V, respectively (V, versus SCE) [88], which suggests that the indenyl monoanion is less electron-donating than the cyclopentadienyl monoanion.

The crystal structure of the fluorenyl complex $[(\eta^5\text{-}C_{13}H_9)Co^{III}(2,3\text{-}C_2B_9H_{11})]$ is available [89].

A series of monocarbon-$[(\eta^5\text{-}C_9H_7)Co^{III}(2\text{-R-}2,3\text{-}C_2B_9H_{10})]$ (R = Ph, CH_2OMe) and dicarbon-substituted $[(\eta^5\text{-}C_9H_7)Co^{III}(2,3\text{-}R_2\text{-}2,3\text{-}C_2B_9H_9)]$ (R = CH_2OMe) derivatives have been crystallographically characterized [90]. The structures of the B-substituted complexes $[(\eta\text{-}C_5H_5)Co^{III}(5\text{-R-}2,3\text{-}C_2B_9H_{10})]$ (R = OC(O)Me, C(O)Me) have also been solved by X-ray [91].

A few half-sandwich cobaltacarboranes in which the capping $[\eta^5\text{-}C_5H_5]^-$ is replaced by $[\eta^5\text{-}NC_4H_4]^-$ have been structurally characterized [92].

8.3.1.1.2. Full-sandwich complexes. It has long been known that $[Co^{III}(2,3\text{-}C_2B_9H_{11})_2]^-$ reversibly undergoes reduction to the corresponding $[Co^{II}(2,3\text{-}C_2B_9H_{11})_2]^{2-}$ (as well as the subsequent Co(II)/Co(I) reduction) [4c]. The crystal structures of the Co(III)/Co(II) redox couple are available [93,94] and a few selected bond distances are compiled in Table 8.

Just as for the cobaltocene/cobaltocenium redox change (and opposite to the ferrocene/ferrocenium couple) [45], the present Co(II)/Co(III) passage is accompanied by shortening of the Co–C_2B_3 bond lengths. In addition, the one-electron transfer triggers rotational cisoid-to-transoid movement, Scheme 8 [94].

A series of complexes substituted at the carbon or at the boron atoms have been characterized.

Let us start with the carbon-monosubstituted complexes $[Co^{III}(2\text{-R-}2,3\text{-}C_2B_9H_{10})_2]^-$ (R = Me, Ph, SEt, $CH_2O(CH_2)_2OMe$ [94–96]). Fig. 12 shows the represenative molecular structure of $[Co^{III}(2\text{-Ph-}2,3\text{-}C_2B_9H_{10})_2]^-$ [96],

Table 8
Selected metal-bond (average) distances (Å) in the Co(III)/Co(II) couple $[Co(2,3\text{-}C_2B_9H_{11})_2]^{-/2-}$

Complex	Co-C2	Co-C3	Co-B4	Co-B5	Co-B6	Reference
$[Co^{III}(2,3\text{-}C_2B_9H_{11})_2]^-$	2.04	2.04	2.09	2.11	2.10	[93a]
$[Co^{II}(2,3\text{-}C_2B_9H_{11})_2]^{2-}$	2.10	2.14	2.11	2.13	2.18	[94]

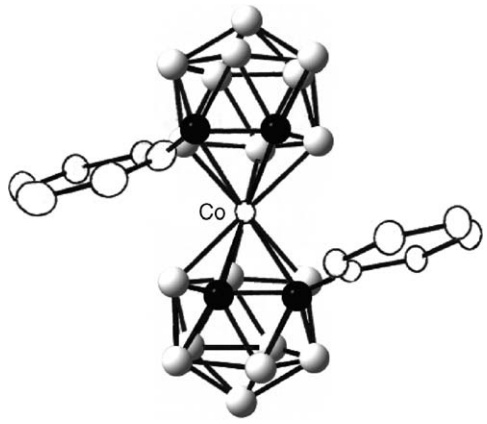

Fig. 12. The molecular structure of $[Co^{III}(2\text{-Ph-}2,3\text{-}C_2B_9H_{10})_2]^-$ (adapted from Ref. [96]).

Table 9
Formal electrode potentials (V, vs. SCE) for the Co(III)/Co(II) reduction of $[Co^{III}(2\text{-R-}2,3\text{-}C_2B_9H_{10})_2]^-$ in MeCN solution

Complex	$E^{\circ\prime}$
$[Co^{III}(2\text{-Me-}2,3\text{-}C_2B_9H_{10})_2]^-$	−0.93
$[Co^{III}(2\text{-Ph-}2,3\text{-}C_2B_9H_{10})_2]^-$	−1.00, −1.28[a]
$[Co^{III}(2\text{-SEt-}2,3\text{-}C_2B_9H_{10})_2]^-$	−0.77
$[Co^{III}(2,3\text{-}C_2B_9H_{11})_2]^-$	−1.07

[a] From Ref. [4a].

but that of $[Co^{III}\{2\text{-}CH_2O(CH_2)_2OMe\text{-}2,3\text{-}C_2B_9H_{10}\}_2]^-$ is also available [94]. Like the unsubstituted complex, the present complexes exhibit chemically reversible reduction to the corresponding Co(II) species, Table 9 [95].

The fact that both the electron-donating Me-substituted complexes reduce at a potential value less negative than the unsubstituted complex, and the electron-withdrawing Ph-substituted complex reduces at a potential value more negative than the Me-substituted complex indicates that the redox potential is not governed by simple inductive effects. The crystal structures of $[(3\text{-}C_4H_8NH\text{-}2,3\text{-}C_2B_9H_{10})Co^{III}(3\text{-}C_4H_8N\text{-}2,3\text{-}C_2B_9H_{10})_2]$ and $[(3\text{-}C_5H_{10}NH\text{-}2,3\text{-}C_2B_9H_{10})Co^{III}(3\text{-}C_5H_{10}N\text{-}2,3\text{-}C_2B_9H_{10})_2]$ are also available [97]. The crystal structure of the two carbon atoms substituted complex $[Co^{III}(2,3\text{-}Et_2\text{-}2,3\text{-}C_2B_9H_9)_2]^-$ is represented in Fig. 13 [95]. As expected, the present complex undergoes the chemically reversible Co(III)/Co(II) reduction. Table 10 summarizes the pertinent electrode potential together with those of related derivatives. Also available is the crystal structure of $[Co^{III}(2,4\text{-}Ph_2\text{-}2,4\text{-}C_2B_9H_9)_2]^-$ [98].

Table 10
Formal electrode potentials (V, vs. SCE) for the Co(III)/Co(II) reduction of the series $[Co^{III}(2\text{-R-}3\text{-R}'\text{-}2,3\text{-}C_2B_9H_9)_2]^-$ in MeCN solution [95]

Complex	$E^{\circ\prime}$
$[Co^{III}(2,3\text{-}Et_2\text{-}2,3\text{-}C_2B_9H_9)_2]^-$	−0.89
$[Co^{III}(2\text{-SEt-}3\text{-Ph-}2,3\text{-}C_2B_9H_9)_2]^-$	−0.66
$[Co^{III}(2\text{-SEt-}3\text{-Me-}2,3\text{-}C_2B_9H_9)_2]^-$	−0.55
$[Co^{III}(2\text{-}\{(CH_2)_2OMe\}\text{-}3\text{-Me-}2,3\text{-}C_2B_9H_9)_2]^-$	−0.86

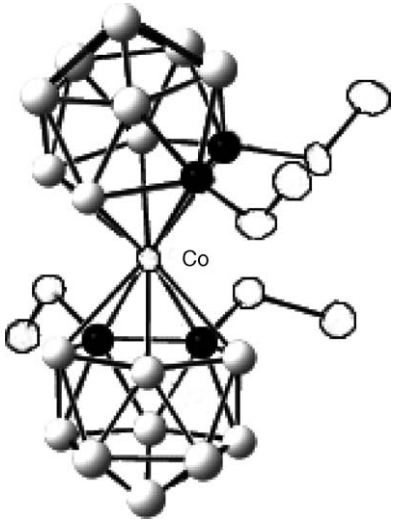

Fig. 13. The molecular structure of $[Co^{III}(2,3\text{-}Et_2\text{-}2,3\text{-}C_2B_9H_9)_2]^-$ (adapted from Ref. [95]).

Let us now pass to the B-substituted cobaltacarboranes. A series of complexes bearing the B-substitution on a single carborane have been crystallographically characterized, namely $[(2,3\text{-}C_2B_9H_{11})Co^{III}(5\text{-R-}2,3\text{-}C_2B_9H_{10})]^-$ [R = I [99], Me, $C_6H_4(CH_2)_3Me$, $(CH_2)_2C_6H_5$ [100], C_6H_5, $O(CH_2CH_2)_2O$ [101], $O(CH_2CH_2O)_2Et$ [102], $O(CH_2CH_2O)C_4H_4N$ [103], $O(CH_2)_2O(CH_2)_2OC_6H_4OMe$ [104]]. As a typical example, Fig. 14 shows the molecular structure of $[(2,3\text{-}C_2B_9H_{11})Co^{III}\{5\text{-}(CH_2)_2C_6H_5)\text{-}2,3\text{-}C_2B_9H_{10}\}]^-$ [100]. The present complexes display the usual reversible Co(III)/Co(II) reduction, Table 11 [100].

Polyoxo appendices present in the structurally characterized $[(2,3\text{-}C_2B_9H_{11})Co^{III}(5\text{-}OCH_2CH_2OR\text{-}2,3\text{-}C_2B_9H_{10}]^-$ (R = C_4H_4N [103], $(CH_2)_2OC_6H_4OMe$ [104]) monoanions proved to be able to electrochemically recognize alkaline or lanthanide ions. The complexes bearing the B-substitution on both the carboranes $[Co^{III}(5\text{-X-}2,3\text{-}C_2B_9H_{10})_2]^-$ (X = Me [105], F [106], Cl [107], I [108]) have been crystallographically characterized. The crystal structure of the substituted complex at two boron atoms of each carborane $[Co^{III}(4,6\text{-}Br_2\text{-}2,3\text{-}C_2B_9H_9)_2]^-$ has been solved [109], as well as that at three boron atoms

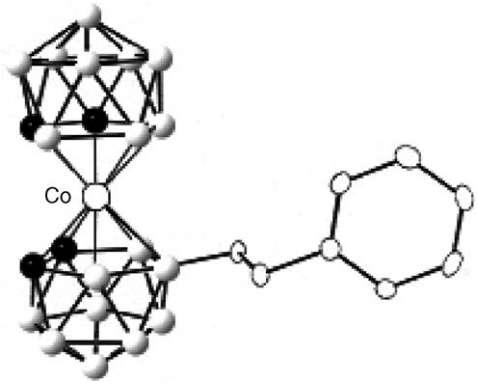

Fig. 14. The molecular structure of $[(2,3\text{-}C_2B_9H_{11})Co^{III}\{5\text{-}(C_2H_4C_6H_5)\text{-}2,3\text{-}C_2B_9H_{10}\}]^-$ (adapted from Ref. [100]).

Table 11
Formal electrode potentials (V, vs. SCE) for the Co(III)/Co(II) reduction of $[(2,3\text{-}C_2B_9H_{11})Co^{III}(5\text{-}R\text{-}2,3\text{-}C_2B_9H_{10})]^-$ in MeCN solution

Complex	$E^{\circ\prime}$
$[(2,3\text{-}C_2B_9H_{11})Co^{III}(5\text{-}I\text{-}2,3\text{-}C_2B_9H_{10})]^-$	−1.20
$[(2,3\text{-}C_2B_9H_{11})Co^{III}(5\text{-}Me\text{-}2,3\text{-}C_2B_9H_{10})]^-$	−1.52
$[(2,3\text{-}C_2B_9H_{11})Co^{III}(5\text{-}Et\text{-}2,3\text{-}C_2B_9H_{10})]^-$	−1.43
$[(2,3\text{-}C_2B_9H_{11})Co^{III}(5\text{-}Ph\text{-}2,3\text{-}C_2B_9H_{10})]^-$	−1.36
$[(2,3\text{-}C_2B_9H_{11})Co^{III}(5\text{-}C_{12}H_9\text{-}2,3\text{-}C_2B_9H_{10})]^-$	−1.39
$[(2,3\text{-}C_2B_9H_{11})Co^{III}(5\text{-}C_{14}H_9\text{-}2,3\text{-}C_2B_9H_{10})]^-$	−1.29
$[(2,3\text{-}C_2B_9H_{11})Co^{III}(5\text{-}C_6H_4Bu\text{-}2,3\text{-}C_2B_9H_{10})]^-$	−1.36
$[(2,3\text{-}C_2B_9H_{11})Co^{III}(5\text{-}C_2H_4C_6H_5\text{-}2,3\text{-}C_2B_9H_{10})]^-$	−1.43

(only one belonging to the C_2B_3 open face) $[Co^{III}(X_3\text{-}2,3\text{-}C_2B_9H_8)_2]^-$ (X = Br [110], Me [111]) have been determined. The electrochemical behavior of the latter bromide complex has been reported [4c].

8.3.1.1.3. Carboranophane complexes. A large number of cobaltacarboranophanes have been crystallographically characterized, in which the bridging group is either B/B or C/C linked, but only few have been electrochemically investigated. Let us start with the B/B bridged derivatives. As a typical example, Fig. 15 illustrates the crystal structure of the pyrazole-bridged $[Co^{III}(2,4\text{-}C_2B_9H_{10})_2\{\mu\text{-}C_3N_2H_3\}]$ [82]. In MeCN solution, it undergoes reversibly the usual sequence Co(III)/Co(II)/Co(I) at $E^{\circ\prime}$ values of −0.59 and −1.80 V, respectively (V, versus SCE) [82], which means that it is more easily reducible that the precursor $[Co^{III}(2,4\text{-}C_2B_9H_{11})_2]^-$ ($E^{\circ\prime} = -1.14$ and −2.52 V [4c]); this depends either on the coulombic effects of the different overall charges or the inductive effects of the bridging group.

Other X-ray characterized B/B bridged complexes are: $[Co(2,3\text{-}C_2B_9H_{10})_2\{\mu\text{-}CH_2\text{-}C_9H_6\}]$ [112], $[Co(2,3\text{-}C_2B_9H_{10})_2\{\mu\text{-}C_6H_4\}]^-$ [113], $[Co(2,3\text{-}C_2B_9H_9)_2\{\mu\text{-}C_6H_4\}_2]^-$ [114], $[Co(2,3\text{-}C_2B_9H_{10})_2\{\mu\text{-}C_3N_2H_2\text{-}5\text{-}COOR\}]$ (R = H [82], R = Me [115]), $[Co(2,3\text{-}C_2B_9H_{10})_2\{\mu\text{-}O\}]^-$ [116], $[Co(2,3\text{-}C_2B_9H_{10})_2\{\mu\text{-}OMe\}]$ [117], $[Co(2,3\text{-}C_2B_9H_{10})_2\{\mu\text{-}S_2\}]^-$ [118], $[Co(2,4\text{-}C_2B_9H_{10})_2\{\mu\text{-}S\}]^-$ [119], $[Co(2,3\text{-}C_2B_9H_{10})_2\{\mu\text{-}SC(H)S\}]$ [120], $[Co(2,3\text{-}C_2B_9H_{10})_2\{\mu\text{-}SCH_2C{\equiv}CH\}]$ [121], $[Co(2,3\text{-}C_2B_9H_{10})_2\{\mu\text{-}SCH_2COOMe\}]$ [122], $[Co(2,3\text{-}C_2B_9H_{10})_2\{\mu\text{-}S_2CH[C_{10}H_5\text{-}2,9\text{-}(NMe_2)_2H]\}]$ [123], $[Co(2,3\text{-}C_2B_9H_{10})_2\{\mu\text{-}SO_4\}]^-$ [101], $[Co(2,4\text{-}C_2B_9H_{10})_2\{\mu\text{-}NHCH_2COOMe\}]$ [124], $[Co(2,4\text{-}C_2B_9H_{10})_2\{\mu\text{-}PMe_2\}]$ [125], $[Co(2,3\text{-}C_2B_9H_{10})_2\{\mu\text{-}CH_3CO_2\}]^-$ [126], $[Co(2,3\text{-}C_2B_9H_{10})_2\{\mu\text{-}PO_3Cl\}]^-$, $[Co(2,3\text{-}C_2B_9H_{10})_2\{\mu\text{-}PO_3NEt_2\}]^-$ [127], $[Co(2,3\text{-}C_2B_9H_{10})_2\{\mu\text{-}C_2H_2\}]^-$ [128].

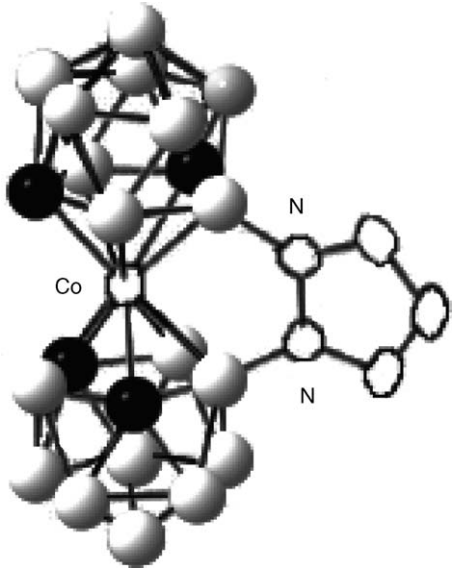

Fig. 15. The molecular structure of $[Co^{III}(2,4\text{-}C_2B_9H_{10})_2\{\mu\text{-}C_3N_2H_3\}]$ (adapted from Ref. [82]).

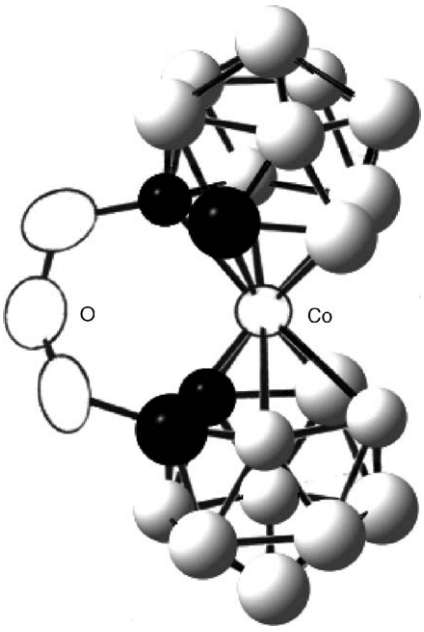

Fig. 16. The molecular structure of $[Co^{III}(2,3\text{-}C_2B_9H_{10})_2\{\mu\text{-}CH_2OCH_2\}]$ (adapted from Ref. [129]).

Let us pass to the C/C bridged derivatives. As a representative example, Fig. 16 outlines the crystal structure of $[Co(2,3\text{-}C_2B_9H_{10})_2\{\mu\text{-}CH_2OCH_2\}]^-$ [129].

In MeCN solution it exhibits the reversible Co(III)/Co(II) reduction at a potential value almost comparable with that of $[Co^{III}(2,3\text{-}C_2B_9H_{11})_2]^-$ [$E^{\circ\prime} = -1.22$ V versus −1.14 V; V, versus SCE)] [129].

Other X-ray characterized C/C bridged complexes are: $[Co(2,3\text{-}C_2B_9H_{10})_2\{\mu\text{-}2,4\text{-}C_3H_6\}]^-$, $[Co(2,3\text{-}C_2B_9H_{10})_2\{\mu\text{-}2,5\text{-}C_4H_8\}]^-$ [81], $[Co(2,3\text{-}C_2B_9H_{10})_2\{\mu\text{-}CH_2SCH_2\}]^-$ [130], and $[Co(2,3\text{-}C_2B_9H_{10})_2\{\mu\text{-}S(CH_2CH_2O)_3CH_2CH_2S\}]^-$ [102]. Finally, the crystal structure of the B/C bridged $[Co(2\text{-}SEt\text{-}3\text{-}Ph\text{-}2,3\text{-}C_2B_9H_9)(2\text{-}Ph\text{-}2,3\text{-}C_2B_9H_{10})\{\mu\text{-}SEt\}]$ is available [131].

8.3.1.2. Charge-compensated complexes.

8.3.1.2.1. Half-sandwich complexes. We have recently reported the electrochemical behavior of the series of charge-compensated complexes illustrated in Scheme 9 [132]. They display the usually reversible sequence Co(III)/Co(II)/Co(I), which, because of either the charge compensation or the inductive effects of the compensating group L, occurs at a poten-

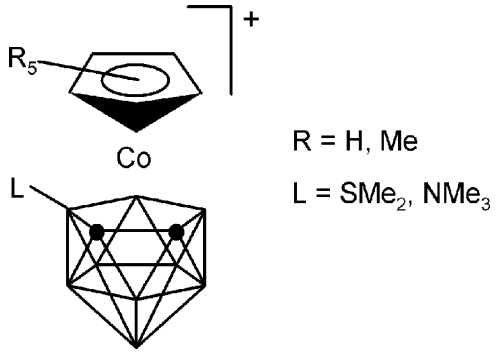

Scheme 9. Structure of a few charge compensated half-sandwich Co(III) derivatives.

Table 12
Formal electrode potentials (V, vs. SCE) for the reduction processes of the monocations $[(C_5R_5)Co(4\text{-}L\text{-}2,3\text{-}C_2B_9H_{10})]^+$ in CH_2Cl_2 solution

Complex	$E^{\circ\prime}_{Co(III)/Co(II)}$	$E^{\circ\prime}_{Co(II)/Co(I)}$
$[(\eta\text{-}C_5Me_5)Co(4\text{-}SMe_2\text{-}2,3\text{-}C_2B_9H_{10})]^+$	−0.91	−1.9[a]
$[(\eta\text{-}C_5H_5)Co(4\text{-}NMe_3\text{-}2,3\text{-}C_2B_9H_{10})]^+$	−0.67	−1.67
$[(\eta\text{-}C_5Me_5)Co(4\text{-}NMe_3\text{-}2,3\text{-}C_2B_9H_{10})]^+$	−0.87	−1.9[a]

[a] Peak-potential for irreversible processes.

tial value notably less negative than that of the classical $[(\eta\text{-}C_5H_5)Co^{III}(2,3\text{-}C_2B_9H_{11})]$, Table 12.

8.3.1.2.2. Full-sandwich complexes. X-ray structure and electrochemistry of the charge-compensated complexes shown in Scheme 10 have been reported [132]. Fig. 17 shows the molecular structures of both $[(2,3\text{-}C_2B_9H_{11})Co(4\text{-}SMe_2\text{-}2,3\text{-}C_2B_9H_{10})]$ and *meso*-$[Co^{III}(6\text{-}SMe_2\text{-}2,3\text{-}C_2B_9H_{10})_2]^+$, this latter being isoelectronic and isostructural with the above mentioned $[Fe^{II}(6\text{-}Me_2S\text{-}2,3\text{-}C_2B_9H_{10})_2]$, Section 8.2.1.2.2. The present complexes also exhibit the expected reversible Co(III)/Co(II)/Co(I) reduction processes. The pertinent formal electrode potentials are compiled in Table 13. The progressive beneficial effect of the charge compensation on the addition of electrons, is well evident.

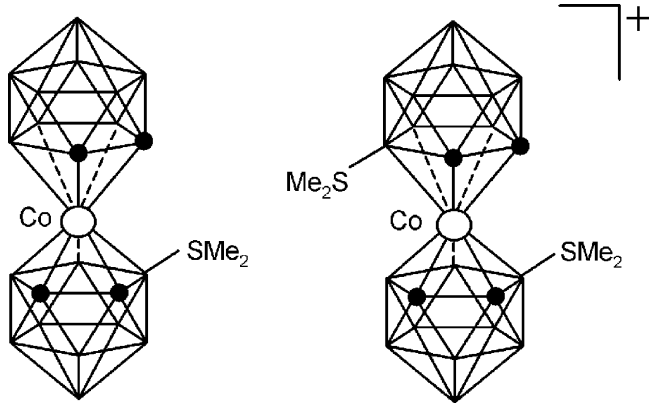

Scheme 10. Structure of a few charge compensated full-sandwich Co(III) derivatives.

Table 13
Formal electrode potentials (V, vs. SCE) for the reduction processes of a few full-sandwich, charge-compensated Co(III) complexes (CH_2Cl_2 solution)

Complex	$E^{\circ\prime}_{Co(III)/Co(II)}$	$E^{\circ\prime}_{Co(II)/Co(I)}$
meso-$[Co^{III}(6\text{-}SMe_2\text{-}2,3\text{-}C_2B_9H_{10})_2]^+$	−0.41	−1.24
$[(2,3\text{-}C_2B_9H_{11})Co(4\text{-}SMe_2\text{-}2,3\text{-}C_2B_9H_{10})]$	−0.89	−1.78
$[Co(2,3\text{-}C_2B_9H_{11})_2]^-$	−1.36[a]	−2.24[a]

[a] MeCN solution; from Ref. [4c].

8.3.2. Rhodacarboranes

8.3.2.1. Classical (charge-noncompensated) complexes.

8.3.2.1.1. Half-sandwich complexes. The X-ray structures of the half-sandwich complexes $[(\eta\text{-}C_5Me_5)Rh(2,3\text{-}C_2B_9H_{11})]$ [133], $[(\eta\text{-}C_5Me_5)Rh(2,3\text{-}Ph_2\text{-}2,3\text{-}C_2B_9H_9)]$ [134], $[(\eta^5\text{-}C_9H_7)Rh(2\text{-}Ph\text{-}2,3\text{-}C_2B_9H_{10})]$ and $[(\eta^5\text{-}C_9H_7)Rh(2,3\text{-}Ph_2\text{-}2,3\text{-}C_2B_9H_9)]$ [135] are available.

8.3.2.1.2. Full-sandwich complexes. The only information of which we are aware concerning full-sandwich rhodacarboranes involves the electrochemical behavior of $[Rh^{III}(2,3\text{-}C_2B_9H_{11})_2]^-$, which shows the Rh(III)/Rh(II)/Rh(I) sequence. At variance with $[Co^{III}(2,3\text{-}C_2B_9H_{11})_2]^-$, however, the Rh(III)/Rh(II) process is partially chemically reversible, whereas the Rh(II)/Rh(I) process is irreversible [4c].

8.3.2.2. Charge-compensated complexes.

8.3.2.2.1. Half-sandwich complexes. The crystal structure of $[(\eta\text{-}C_5Me_5)Rh(4\text{-}SMe_2\text{-}2,3\text{-}C_2B_9H_{10})]^+$ has been solved [136].

8.3.3. Iridacarboranes

8.3.3.1. Classical (charge-noncompensated) complexes.

8.3.3.1.1. Half-sandwich complexes. The X-ray structure of the half-sandwich complexes $[(\eta\text{-}C_5Me_5)Ir(2,3\text{-}C_2B_9H_{11})]$ [133] is known.

8.4. Group 10 metallacarboranes

8.4.1. Nickelacarboranes

8.4.1.1. Classical (charge-noncompensated) complexes.

8.4.1.1.1. Half-sandwich complexes. The electrochemical behavior of $[(\eta\text{-}C_5H_5)Ni^{III}(2,3\text{-}C_2B_9H_{11})]$ has been reported [4c].

8.4.1.1.2. Full-sandwich complexes. Fig. 18 schematizes the crystal structure of $[Ni^{IV}(2,3\text{-}C_2B_9H_{11})_2]$ [137]. In MeCN solution it reversibly undergoes the stepwise sequence Ni(IV)/Ni(III)/Ni(II)/Ni(I) [4c]. The crystal structure of $[Ni^{III}(2,3\text{-}C_2B_9H_{11})_2]^-$ [66a,74b,138] is available. In this connection, as deducible from Table 14, which compiles

Table 14
Selected metal-bond (average) distances (Å) in the Ni(IV)/Ni(III) couple $[Ni(2,3\text{-}C_2B_9H_{11})_2]^{0/-}$

Complex	Ni-C2	Ni-C3	Ni-B4	Ni-B5	Ni-B6	Reference
$[Ni^{IV}(2,3\text{-}C_2B_9H_{11})_2]^0$	2.08	2.07	2.09	2.11	2.10	[137a]
$[Ni^{III}(2,3\text{-}C_2B_9H_{11})_2]^-$	2.14	2.09	2.15	2.11	2.14	[66a]

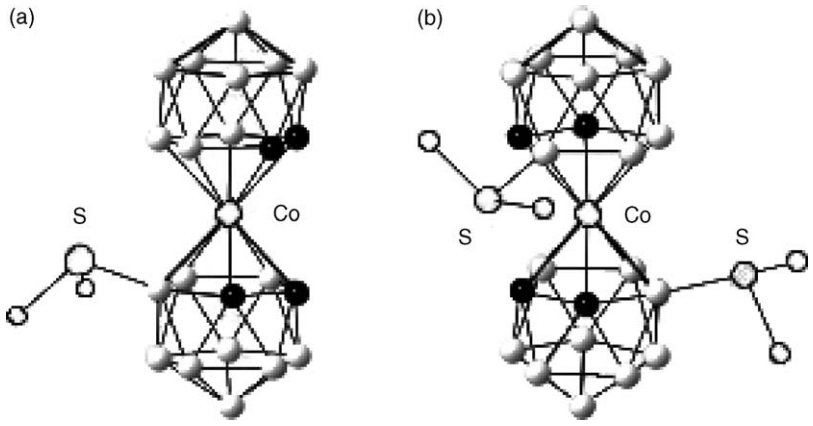

Fig. 17. The molecular structures of: (a) [(2,3-$C_2B_9H_{11}$)Co(4-SMe_2-2,3-$C_2B_9H_{10}$)] and (b) *meso*-[Co^{III}(6-SMe_2-2,3-$C_2B_9H_{10})_2]^+$ (adapted from Ref. [132]).

a few structural data pertinent to the redox couple, the Ni(IV)/Ni(III) passage is not only accompanied by a general elongation of the Ni-ligand distances, but also from the mutual cisoid-to-transoid rotation of the dicarbollide ligands [138a].

It has been noted [139] that such a rotation could be exploited as a molecular motor (in some cases the rotation appears to be partial, based on solid state molecular structures [66a,74b,138b]).

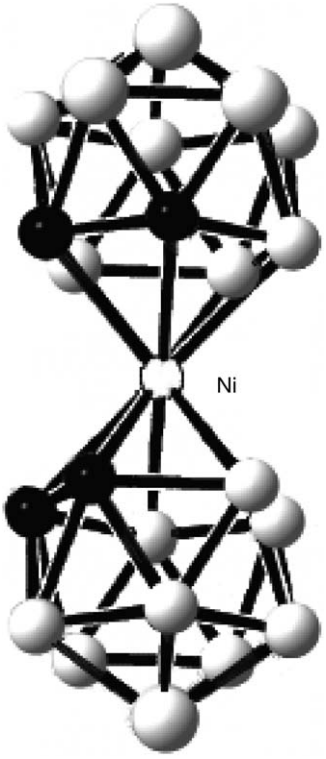

Fig. 18. The molecular structure of [Ni^{IV}(2,3-$C_2B_9H_{11})_2$] (adapted from Ref. [137]).

The crystal structures of [Ni^{II}(2,4-$C_2B_9H_{11})_2]^{2-}$ [140] and of the symmetrically substituted [5-OMe-Ni^{IV}(2,3-$C_2B_9H_9)_2]^0$ [141] and the asymmetrically substituted [Ni^{IV}(Me_2-2,3-$C_2B_9H_9$)(Me_2-2′,6′-$C_2B_9H_9$)]^0 [142] are also known. The isomers [Ni^{IV}(2,3-$C_2B_9H_{11})_2$] and [Ni^{III}(2,4-$C_2B_9H_{11})_2]^-$ undergo the sequence Ni(IV)/Ni(III)/Ni(II)/Ni(I) at rather different potential values (see the next Table 15) [4c].

8.4.1.1.3. Carboranophane complexes. As in the case of Fe and Co complexes, B/B and C/C nickelacarboranophanes have been prepared. In particular, the B/B linked [Ni^{III}(2,4-$C_2B_9H_{10})_2${μ-$C_3N_2H_3$}] [82] and the C/C linked [2,3′-μ-(C_4H_8)-Ni^{III}(2,3-$C_2B_9H_{10})_2]^-$ [81] have been X-ray characterized. In MeCN solution, [Ni^{III}(2,4-$C_2B_9H_{10})_2${μ-$C_3N_2H_3$}] exhibits the reversible sequence Ni(IV)/Ni(III)/Ni(II)/Ni(I) [82]; Table 15.

8.4.1.2. Charge-compensated complexes.

8.4.1.2.1. Half-sandwich complexes. Fig. 19 shows the cyclic voltammetric behavior of [(η-C_5H_5)Ni^{II}(6-SMe_2-2,3-$C_2B_9H_{10}$)] in CH_2Cl_2 solution [143]. It undergoes two separated, chemically reversible, one-electron oxidation processes [which involve the sequence Ni(II)/Ni(III)/Ni(IV)] and the Ni(II)/Ni(I) reduction, the latter process being complicated by following chemical reactions (at high scan rates the coupled chemical reactions can be partially prevented). Table 16 compares the formal electrode potentials of such redox changes with those of the classical analogue.

As previously cited (Sections 8.2.1.2.1, 8.2.1.2.2, 8.2.2.2.1, 8.3.1.2.), also in this case the charge compensation causes a

Table 15
Formal electrode potentials (V, vs. SCE) for the redox changes of the nickelacarboranophane [Ni^{III}(2,3-$C_2B_9H_{10})_2${μ-$C_3N_2H_3$}] in MeCN solution

Complex	$E^{\circ\prime}_{Ni(IV)/Ni(III)}$	$E^{\circ\prime}_{Ni(III)/Ni(II)}$	$E^{\circ\prime}_{Ni(II)/Ni(I)}$
[Ni^{III}(2,4-$C_2B_9H_{10})_2$ {μ-$C_3N_2H_3$}]	+1.56	−0.19	−1.76
[Ni(2,4-$C_2B_9H_{11})_2]^-$	+0.55	−0.92	−2.09
[Ni(2,3-$C_2B_9H_{11})_2]^-$	+0.25	−0.57	−2.10

Table 16
Formal electrode potentials (V, vs. SCE) for the redox changes of $[(\eta\text{-}C_5H_5)Ni^{II}(6\text{-}SMe_2\text{-}2,3\text{-}C_2B_9H_{10})]$

Complex	$E^{\circ\prime}_{Ni(IV)/Ni(III)}$	$E^{\circ\prime}_{Ni(III)/Ni(II)}$	$E^{\circ\prime}_{Ni(II)/Ni(I)}$	Solvent
$[(\eta\text{-}C_5H_5)Ni^{II}(6\text{-}SMe_2\text{-}2,3\text{-}C_2B_9H_{10})]$	+1.11	+0.14	−1.48[a]	CH_2Cl_2
$[(\eta\text{-}C_5H_5)Ni^{III}(2,3\text{-}C_2B_9H_{11})]$	+0.55	−0.52	–	MeCN

[a] Coupled to chemical reactions; measured at high scan rate.

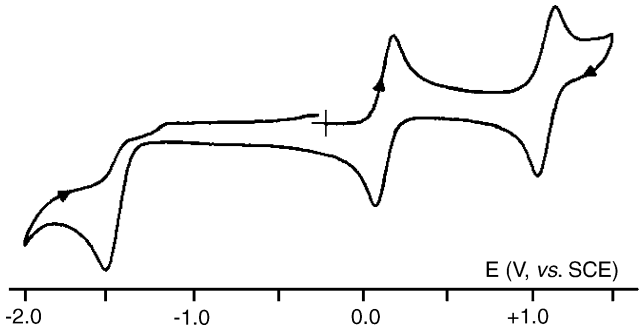

Fig. 19. Cyclic voltammogram recorded at a platinum electrode in CH_2Cl_2 solution of $[(\eta\text{-}C_5H_5)Ni^{II}(6\text{-}SMe_2\text{-}2,3\text{-}C_2B_9H_{10})]$. Scan rate 0.2 V s^{-1} (from Ref. [143]).

significant shift of the Ni(IV)/Ni(III)/Ni(II) sequence towards positive potential values thus allowing access to the Ni(II)/Ni(I) process.

8.4.1.2.2. Full-sandwich complexes. Fig. 20 shows the solid-state structure of *meso*-$[Ni^{II}(6\text{-}SMe_2\text{-}2,3\text{-}C_2B_9H_{10})_2]$ [143]. As illustrated in Fig. 21, the Ni(II) complex exhibits the reversible four-membered sequence Ni(IV)/Ni(III)/Ni(II)/Ni(I) [143]. The pertinent redox potentials are compiled in Table 17.

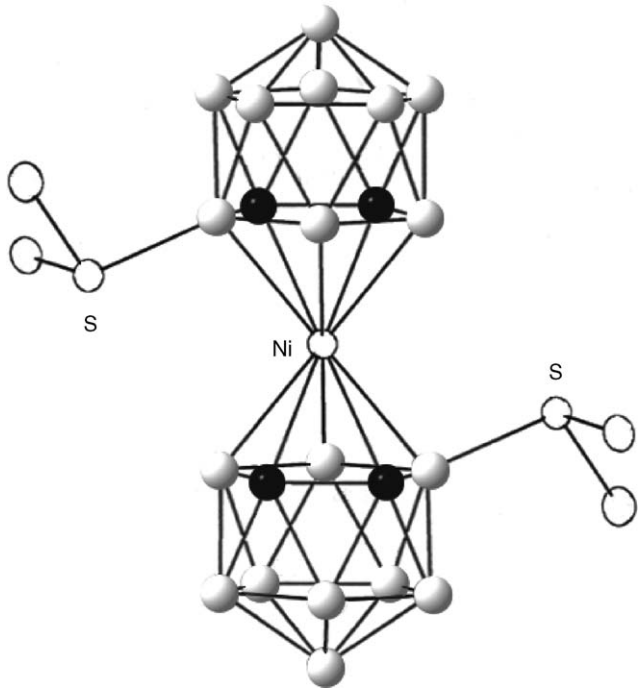

Fig. 20. The molecular structure of *meso*-$[Ni^{II}(6\text{-}SMe_2\text{-}2,3\text{-}C_2B_9H_{10})_2]$ (from Ref. [143]).

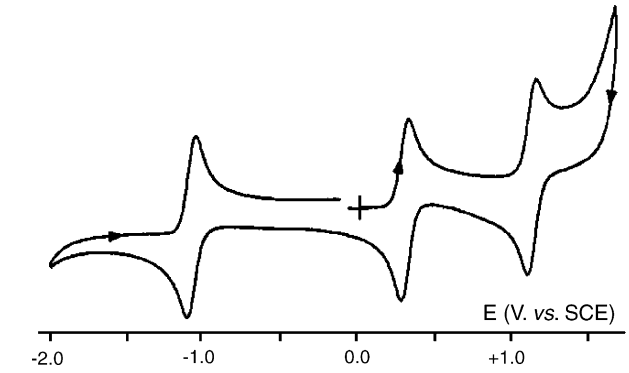

Fig. 21. Cyclic voltammogram recorded at a platinum electrode in CH_2Cl_2 solution of *meso*-$[Ni^{II}(6\text{-}SMe_2\text{-}2,3\text{-}C_2B_9H_{10})_2]$. Scan rate 0.2 V s^{-1} (from Ref. [143]).

8.5. Group 11 metallacarboranes

8.5.1. Cupracarboranes

8.5.1.1. Classical (charge-noncompensated) complexes.

8.5.1.1.1. Full-sandwich complexes. Fig. 22 shows a schematic picture of $[Cu^{III}(2,3\text{-}C_2B_9H_{11})_2]^-$ [144].

At variance with the symmetrical structure of the previous full-sandwich complexes, the copper complex has a slipped sandwich structure, which substantially makes the copper ion

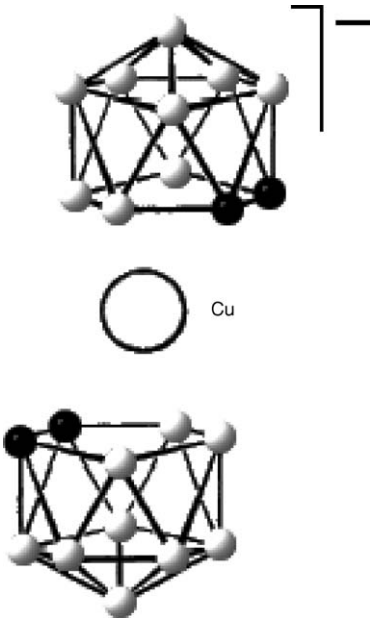

Fig. 22. The molecular structure of $[Cu^{III}(2,3\text{-}C_2B_9H_{11})_2]^-$ (adapted from Ref. [144]).

Table 17
Formal electrode potentials (V, vs. SCE) for the redox changes of $[Ni^{II}(6\text{-}SMe_2\text{-}2,3\text{-}C_2B_9H_{10})_2]$

Complex	$E^{\circ\prime}_{Ni(IV)/Ni(III)}$	$E^{\circ\prime}_{Ni(III)/Ni(II)}$	$E^{\circ\prime}_{Ni(II)/Ni(I)}$	Solvent
$[Ni^{II}(6\text{-}SMe_2\text{-}2,3\text{-}C_2B_9H_{10})_2]$	+1.17	+0.35	−1.06	CH_2Cl_2
$[Ni^{IV}(2,3\text{-}C_2B_9H_{11})_2]$[a]	+0.25	−0.57	−2.10	MeCN

[a] From Ref. [4c].

Table 18
Selected metal-bond (average) distances (Å) in the Cu(III)/Cu(II) couple $[Cu(2,3\text{-}C_2B_9H_{11})_2]^{-/2-}$

Complex	Cu-C2	Cu-C3	Cu-B4	Cu-B5	Cu-B6
$[Cu^{III}(2,3\text{-}C_2B_9H_{11})_2]^-$	2.50	2.51	2.17	2.15	2.05
$[Cu^{II}(2,3\text{-}C_2B_9H_{11})_2]^{2-}$	2.58	2.57	2.21	2.13	2.25

essentially coordinate to the vicinal three B atoms of each C_2B_9 ligand. In MeCN solution the monoanion exhibits reversible reduction to the corresponding Cu(II) dianion [4c]. As a matter of fact, the dianion $[Cu^{II}(2,3\text{-}C_2B_9H_{11})_2]^{2-}$ substantially maintains the slipped structure of the Cu(III) precursor [145], with a general elongation of the Cu-C_2B_3 distances with respect to the monoanion, Table 18.

8.5.1.1.2. Carboranophane complexes. Fig. 23 illustrates the crystal structure of the B/B pyrazole-bridged $[Cu^{III}(2,4\text{-}C_2B_9H_{10})_2\{\mu\text{-}C_3N_2H_3\}]$ [82]. As seen, the constraints imposed by the bridge prevent the slipping of the two carborane halves present in the full-sandwich Cu(III) derivative. In MeCN solution, $[Cu^{III}(2,4\text{-}C_2B_9H_{10})_2\{\mu\text{-}C_3N_2H_3\}]$ exhibits the reversible sequence Cu(III)/Cu(II)/Cu(I) ($E^{\circ\prime}_{Co(III)/Co(II)} = -0.08$ V; $E^{\circ\prime}_{Co(II)/Co(I)} = -0.72$ V; V, versus SCE) [82].

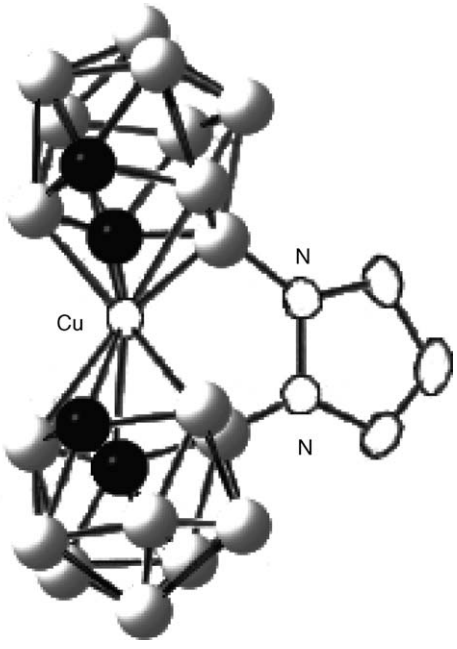

Fig. 23. The molecular structure of $[Cu^{III}(2,4\text{-}C_2B_9H_{10})_2\{\mu\text{-}C_3N_2H_3\}]$ (adapted from Ref. [82]).

8.5.2. Auracarboranes

8.5.2.1. Classical (charge-noncompensated) complexes.

8.5.2.1.1. Full-sandwich complexes. The crystal structure of $[Au^{III}(2,3\text{-}C_2B_9H_{11})_2]^-$ is known [146]. It exhibits the slipped asymmetric deviation already discussed for $[Cu(2,3\text{-}C_2B_9H_{11})_2]^{n-}$. In MeCN solution it undergoes the reversible sequence Au(III)/Au(II)/Au(I) [4c]. The same structural distorsion is obviously present in $[Au^{III}(2,3\text{-}Me_2\text{-}2,3\text{-}C_2B_9H_9)_2]^-$ [147].

9. CPB_9 cages

9.1. Group 8 metallacarboranes

9.1.1. Ferraphosphacarboranes

9.1.1.1. Full-sandwich complexes. The crystal structure of $[Fe^{II}(5\text{-}Me\text{-}2,5\text{-}CPB_9H_{10})_2]$ is available [148] together with the its electrochemistry and those of related derivatives [4c].

9.2. Group 9 metallacarboranes

9.2.1. Cobaltaphosphacarboranes

9.2.1.1. Full-sandwich complexes. The electrochemistry of a series of $[Co^{III}(CPB_9H_{10})_2]^-$ derivatives has been reviewed [4c].

10. C_3B_2 cages

10.1. Group 8 metallacarboranes

10.1.1. Ferracarboranes

10.1.1.1. Half-sandwich complexes. Fig. 24 exemplifies the crystal structure of $[(\eta\text{-}C_5Me_5)Fe^{III}\{2\text{-}Me\text{-}4,5\text{-}Pr^i_2\text{-}3,6\text{-}Et_2\text{-}2,4,5\text{-}C_3B_2\}]$ [149]. The C_3B_2 face is highly distorted from the planar geometry. In DME solution it reversibly undergoes Fe(III)/Fe(II) reduction ($E^{\circ\prime} = -1.26$ V, versus SCE) [149b].

10.1.2. Ruthenacarboranes

10.1.2.1. Half-sandwich complexes. In DME solution, complex $[(\eta\text{-}C_5Me_5)Ru^{III}\{2\text{-}Me\text{-}4,5\text{-}Et_2\text{-}3,6\text{-}Bu^t_2\text{-}2,4,5\text{-}C_3B_2\}]$ exhibits reversible Ru(III)Ru(II) reduction ($E^{\circ\prime} = -1.40$ V, versus SCE). [149b].

10.2. Group 9 metallacarboranes

10.2.1. Cobaltacarboranes

10.2.1.1. Half-sandwich complexes. The crystal structures of $[(\eta\text{-}C_5H_5)Co^{III}(2\text{-}Me\text{-}4,5\text{-}Et_2\text{-}3,6\text{-}Et_2\text{-}2,4,5\text{-}C_3B_2)]$ [150]

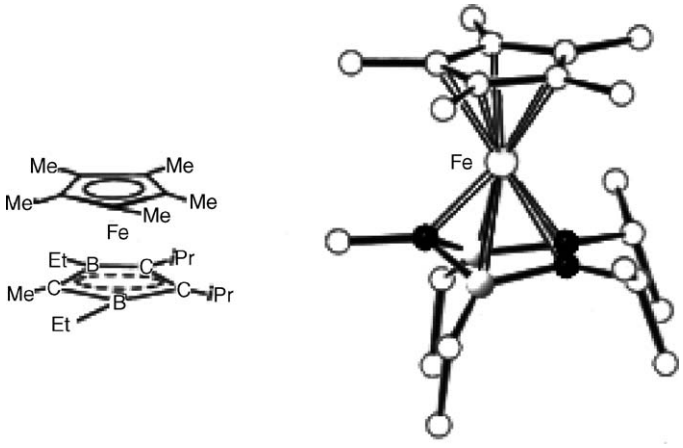

Fig. 24. The molecular structure of [(η-C_5Me_5)Fe^{III}{2-Me-4,5-Pr^i_2-3,6-Et_2-2,4,5-C_3B_2}] (adapted from Ref. [149]).

and [(η-C_5H_5)Co^{III}(η^5-1,2,3-trimethyl-decahydro-1,3-dibora-cyclopentacyclooctene)] [151] are known.

10.3. Group 10 metallacarboranes

10.3.1. Nickelacarboranes

10.3.1.1. Half-sandwich complexes. The crystal structures of [(η-C_5H_5)Ni^{III}(2-Me-4,5-Et_2-3,6-Et_2-2,4,5-C_3B_2)] [152] and [(η-C_5H_5)Ni^{III}(η^5-1,2,3-trimethyl-decahydro-1,3-dibora-cyclopentacyclooctene)] [151] are available.

10.3.1.2. Full-sandwich complexes. The crystal structure of [Ni^{III}(4,5-Me_2-3,6-Me_2-2,4,5-$C_3B_2H)_2$] is available [150b].

11. C_3B_3 cages

11.1. Group 10 metallacarboranes

11.1.1. Nickelacarboranes

11.1.1.1. Half-sandwich complexes. Fig. 25 shows the solid-state molecular structure of the unconventional (C_3B_2-capped) half-sandwich [(2,3-Et_2-4,6-Me_2-2,3,5-C_3B_2)Ni(2,3-Et_2-4,6,7-Me_3-2,3,5-C_3B_3)] [153]. In DME solution it undergoes a chemically reversible (in the cyclic voltammetric time scale) reduction to the corresponding monoanion ($E^{\circ\prime} = -1.47$ V, versus SCE) [153].

11.1.1.2. Full-sandwich complexes. Fig. 26 stands for the X-ray structure of [Ni^{III}(2,3-Et_2-4,6,7-Me_3-2,3,5-$C_3B_3)_2$] [154]. In CH_2Cl_2 solution it undergoes a chemically reversible oxidation to the corresponding monocation ($E^{\circ\prime} = -0.11$ V, versus SCE).

12. C_3B_8 cages

The chemistry of the 11-vertex tricarbollide monoanions [*nido*-$C_{3-x}P_xB_8H_{11-x}$]$^-$ ($x = 0$–2) (carbons adjacent or apart) is rapidly expanding [155] and, in consequence of their analogy with [C_5H_5]$^-$, afford a mononegative substitute for the

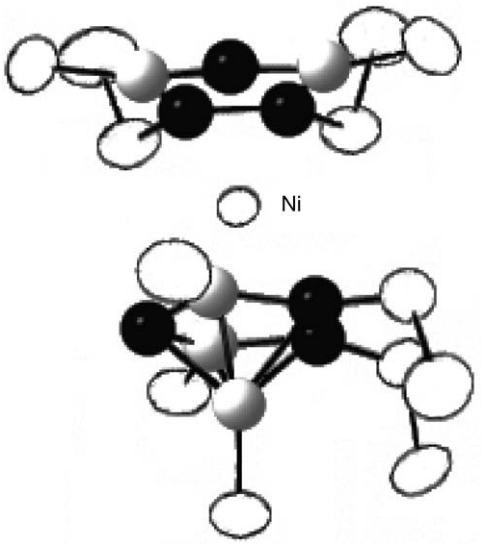

Fig. 25. The molecular structure of [(2,3-Et_2-4,6-Me_2-2,3,5-C_3B_2)Ni(2,3-Et_2-4,6,7-Me_3-2,3,5-C_3B_3)] (adapted from Ref. [153]).

dicarbollide dianion [*nido*-$C_2B_9H_{11}$]$^{2-}$, that can replace it in metallacarboranes analogues of metallocenes.

12.1. Group 8 metallacarboranes

12.1.1. Ferracarboranes

12.1.1.1. Half-sandwich complexes. Fig. 27 shows the crystal structure of [(η-C_5H_5)Fe^{II}(2,3,4-$C_3B_8H_{11}$)] [156]. As illustrated in Fig. 28, in CH_2Cl_2 solution it undergoes reversibly the Fe(II)/Fe(III) oxidation at potential values notably higher than that of the dicarbollide analogue [69].

It is noted that in spite of the apparent chemical reversibility of the oxidation process in the short times of cyclic

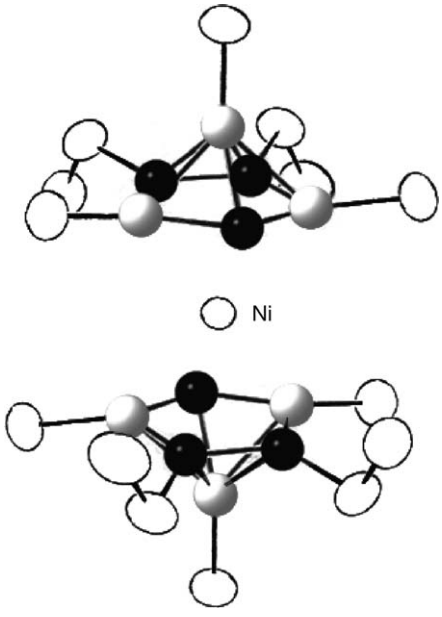

Fig. 26. The molecular structure and of [Ni^{III}{2,3-Et_2-4,6,7-Me_3-2,3,5-C_3B_3}$_2$] (adapted from Ref. [154]).

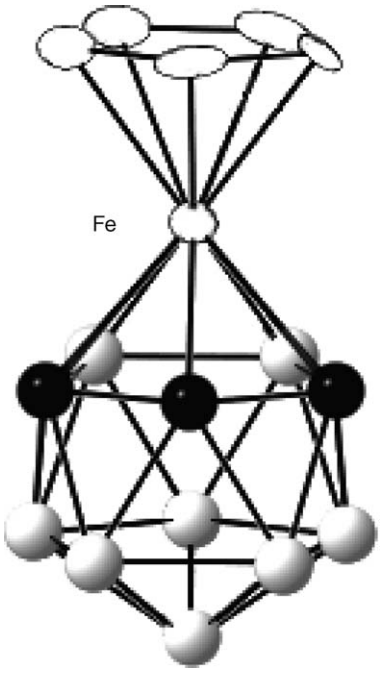

Fig. 27. The molecular structure of $[(\eta\text{-}C_5H_5)Fe^{II}(2,3,4\text{-}C_3B_8H_{11})]$ (adapted from Ref. [156]).

voltammetry, exhaustive oxidation triggers partial decomposition of $[(\eta\text{-}C_5H_5)Fe^{III}(2,3,4\text{-}C_3B_8H_{11})]^+$ [69]. Similar behavior is exhibited by the crystallographically characterized derivatives $[(\eta\text{-}C_5H_5)Fe^{II}(2,3,5\text{-}C_3B_8H_{11})]$ [156] and $[(\eta\text{-}C_5H_5)Fe^{II}(12\text{-}NHBu^t\text{-}2,4,12\text{-}C_3B_8H_{10})]$ [157] (12 indicates the apical carbon atom opposite to the C_2B_3 coordinating pentagonal face), even if in these cases the oxidised Fe(III) derivative is stable.

As happens for the related Ni complexes (Section 8.4.1.2), the high potential value of the Fe(II)/Fe(III) oxidation provides, in some cases, access to the Fe(II)/Fe(I) reduction, which becomes more readily detectable in THF solvent due to its wide cathodic window, Fig. 29. The pertinent redox potentials are compiled in Table 19 [69].

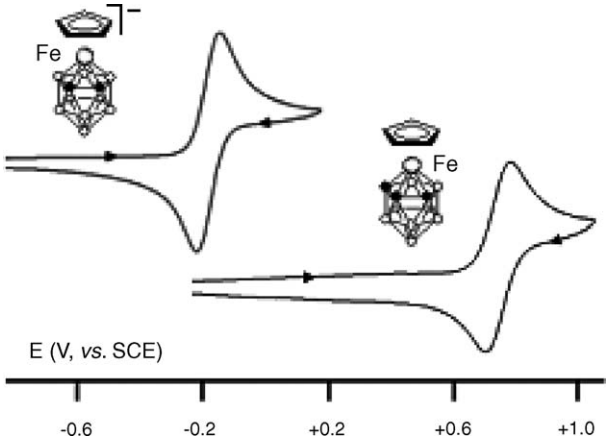

Fig. 28. Comparison between the cyclic voltammetric behavior of $[(\eta\text{-}C_5H_5)Fe^{II}(2,3,4\text{-}C_3B_8H_{11})]$ and that of $[(\eta\text{-}C_5H_5)Fe^{II}(2,3\text{-}C_2B_9H_{11})]^-$ in CH_2Cl_2 solution. Platinum working electrode. Scan rate 0.2 V s^{-1} (from Ref. [69]).

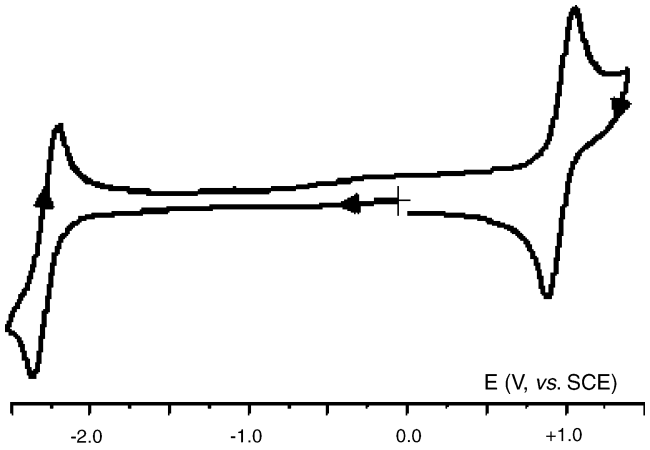

Fig. 29. Cyclic voltammetric response recorded at a gold electrode in THF solution of $[(\eta\text{-}C_5H_5)Fe^{II}(2,4,7\text{-}C_3B_8H_{11})]$. Scan rate 0.2 V s^{-1} (from Ref. [69]).

These data clearly reveal how the position of the cage carbon atoms (adjacent versus non-adjacent) plays an appreciable role in determining the redox potential, suggesting that electrochemistry can provide an additional simple tool, which can supplement the usual NMR and X-ray techniques in distinguishing different metalla-tricarbollide isomers. Further crystallographically characterized half-sandwich complexes are: $[(\eta\text{-}C_5H_5)Fe^{II}(7\text{-}NHBu^t\text{-}1,4,7\text{-}C_3B_8H_{10})]$ [158] $[(\eta\text{-}C_5H_5)Fe^{II}(9\text{-}NHBu^t\text{-}2,7,9\text{-}C_3B_8H_{10})]$, $[(\eta\text{-}C_5H_5)Fe^{II}(10\text{-}NHBu^t\text{-}2,7,10\text{-}C_3B_8H_{10})]$, and $[(\eta\text{-}C_5H_5)Fe^{II}(4\text{-}NHBu^t\text{-}2,4,7\text{-}C_3B_8H_{10})]$ [17g].

12.1.1.2. Full-sandwich complexes. A number of full-sandwich ferra-tricarbollides bearing a amino substituent at one of the carbon atom have been crystallographic characterized [namely, $[Fe^{II}(12\text{-}R\text{-}2,4,12\text{-}C_3B_8H_{10})_2]$ (R = $NHBu^t$ [159], NH_2 [160]) and $[(12\text{-}R\text{-}2,4,12\text{-}C_3B_8H_{10})Fe^{II}(7\text{-}R\text{-}2,4,7\text{-}C_3B_8H_{10})]$ (R = $NHBu^t$ [160]); 7 indicates the carbon atom residing in the CB_4 plane below the C_2B_3 coordinating pentagonal face], but no electrochemical data are presently available.

12.1.2. Ruthenacarboranes

12.1.2.1. Half-sandwich complexes. The crystal structures of $[(\eta\text{-}C_5Me_5)Ru^{II}(2,4,7\text{-}C_3B_8H_{11})]$ [156] and $[(\eta\text{-}C_5Me_5)Ru^{II}(12\text{-}R\text{-}2,3,12\text{-}C_3B_8H_{10})]$ (R = $NHBu^t$) [161] are known.

12.1.2.2. Full-sandwich complexes. The crystal structure of $[Ru^{II}(12\text{-}R\text{-}2,4,12\text{-}C_3B_8H_{10})_2]$ (R = $NHBu^t$) is available [159].

13. C_2PB_8 cages

13.1. Group 8 metallacarboranes

13.1.1. Ferracarboranes

13.1.1.1. Half-sandwich complexes. The crystal structure of $[(\eta\text{-}C_5H_5)Fe^{II}(2,3,5\text{-}C_2PB_8H_{10})]$ is available [162].

Table 19
Formal electrode potentials (V, vs. SCE) for the Fe(II)/Fe(III) passage in half-sandwich ferra-tricarbollide complexes

Complex	$E^{\circ\prime}_{Fe(III)/Fe(II)}$	$E^{\circ\prime}_{Fe(II)/Fe(I)}$	Solvent
$[(\eta\text{-}C_5H_5)Fe^{II}(2,3,4\text{-}C_3B_8H_{11})]$	+0.74	−1.80[a]	CH_2Cl_2
	+0.91	−1.56	THF
$[(\eta\text{-}C_5H_5)Fe^{II}(2,3,5\text{-}C_3B_8H_{11})]$	+0.82	−1.56	CH_2Cl_2
	+0.94	−2.05[a]	THF
$[(\eta\text{-}C_5H_5)Fe^{II}(2,4,7\text{-}C_3B_8H_{11})]$	+0.80	–	CH_2Cl_2
	+0.96	−2.29	THF
$[(\eta\text{-}C_5H_5)Fe^{II}(12\text{-}NHBu^t\text{-}2,4,12\text{-}C_3B_8H_{10})]$	+0.60	–	CH_2Cl_2
$[(\eta\text{-}C_5H_5)Fe^{III}(2,3\text{-}C_2B_9H_{11})]$	−0.18	–	CH_2Cl_2

[a] Peak-potential value for irreversible processes.

14. CP_2B_8 cages

14.1. Group 8 metallacarboranes

14.1.1. Ferracarboranes

14.1.1.1. Half-sandwich complexes. The crystal structure of $[(\eta\text{-}C_5H_5)Fe^{II}(2,4,5\text{-}CP_2B_8H_9)]$ is available [163].

15. C_4B_7 cages

As illustrated in Ref. [14], the C_4B_7 cage can assume hapticity different from pentacoordination.

15.1. Group 9 metallacarboranes

15.1.1. Cobaltacarboranes

15.1.1.1. Half-sandwich complexes. The crystal structures of $[(\eta\text{-}C_5H_5)Co(Me_4\text{-}C_4B_7H_7)]$ [164] and $[(\eta\text{-}C_5H_5)Co(Me_4\text{-}OEt\text{-}C_4B_7H_6)]$ [165] have been solved (in both cases, two Me groups are linked to the coordinating C_2B_3 pentagonal face).

16. Conclusions

The chemistry of metallacarborane sandwich complexes is in continuous expansion, but, in contrast to metallocene chemistry, which has been explored by many research groups, it is still the dominion of a relatively limited number of highly specialized research groups. The aim of the present review is not only to point out this aspect, but also to underline that the study of their electrochemistry, which in metallocenes is nowdays considered a necessary tool to exploit their fundamental and applicative capacities, has been largely under-utilised.

Acknowledgements

We are greatly indebted to R.N. Grimes (University of Virginia, Charlottesville, USA) and A.R. Kudinov (A.N. Nesmeyanov Institute of Organoelement Compounds, Moscow, Russian Federation), who made it possible for us to explore this field of chemistry. The financial support of the University of Siena is gratefully acknowledged.

References

[1] M.F. Hawthorne, D.C. Young, P.A. Wegner, J. Am. Chem. Soc. 87 (1965) 1818.
[2] A few recent review papers;
(a) M.F. Hawthorne, Pure Appl. Chem. 63 (1991) 327;
(b) R.N. Grimes, Chem. Rev. 92 (1992) 251;
(c) R.N. Grimes, Coord. Chem. Rev. 143 (1995) 71;
(d) E.W. Abel, F.G.A. Stone, G. Wilkinson (Eds.), Comprehensive Organometallic Chemistry II, Pergamon Press, Oxford, 1995 (Chapters 6–9);
(e) A.K. Saxena, J.A. Maguire, N.S. Hosmane, Chem. Rev. 97 (1997) 2421;
(f) M.F. Hawthorne, A. Maderna, Chem. Rev. 99 (1999) 3421;
(g) R.N. Grimes, in: F.A. Cotton, G. Wilkinson, C.A. Murillo, M. Bochmann (Eds.), Advanced Inorganic Chemistry, sixth ed., Wiley Interscience, NY, 1999 (Chapter 5);
(h) I.B. Sivaev, V.I. Bregadze, Collect. Czech. Chem. Commun. 64 (1999) 783;
(i) R.N. Grimes, Coord. Chem. Rev. 200–202 (2000) 773;
(l) R.N. Grimes, Collect. Czech. Chem. Commun. 67 (2002) 728;
(m) Z. Xie, Coord. Chem. Rev. 231 (2002) 23;
(n) N.S. Hosmane, J.A. Maguire, Organometallics 24 (2005) 1356.
[3] A.H. Soloway, W. Tjarks, B.A. Barnum, F.-G. Rong, R.F. Barth, I.M. Codogni, J.G. Wilson, Chem. Rev. 98 (1998) 1515.
[4] (a) M.F. Hawthorne, D.C. Young, T.D. Andrews, D.V. Howe, R.L. Pilling, A.D. Pitts, M. Reintjes, L.F. Warren Jr., P.A. Wegner, J. Am. Chem. Soc. 90 (1968) 879;
(b) M.F. Hawthorne, G.B. Dunks, Science 78 (1972) 462;
(c) W.E. Geiger Jr., in: R.N. Grimes (Ed.), Metal Interactions with Boron Clusters, Plenum Press, NY, 1982 (Chapter 6);
(d) R.N. Grimes, J. Organomet. Chem. 581 (1999) 1.
[5] *Hexahapto*-CB_9. Rh-complexes: E.J. Ditzel, X.L.R. Fontaine, N.G. Greenwood, J.D. Kennedy, Z. Sisan, B. Štíbr, M. Thornton-Pett, J. Chem. Soc. Chem. Commun. (1990) 1741.
[6] *Tetrahapto*-C_2B_6. Rh-complexes: M.G.S. Londesborough, Z. Janoušek, B. Štíbr, I. Ćisařová, J. Organomet. Chem. 689 (2004) 2702.
[7] *Tetrahapto*-C_2B_8. Ni-complexes: G.K. Barker, N.R. Godfrey, M. Green, H.E. Parge, F.G.A. Stone, A.J. Welch, J. Chem. Soc. Chem. Commun. (1983) 277.
[8] *Hexahapto*-C_2B_8. Co-complexes: L.I. Zakharkin, L.I. Kanakhina, A.I. Yanovsky, V.A. Antonovich, Yu.T. Struchkov, Koord. Khim. (Russ.) 7 (1981) 1692.
[9] Rh-complexes;
(a) Ref. [5];
(b) M. Bown, B. Grüner, B. Štíbr, X.L.R. Fontaine, M. Thornton-Pett, J.D. Kennedy, J. Organomet. Chem. 614–615 (2000) 269.
[10] *Hexahapto*-C_2B_{10}. Ti-complexes: F.Y. Lo, C.E. Strouse, K.P. Callahan, C.B. Knobler, M.F. Hawthorne, J. Am. Chem. Soc. 97 (1975) 428.

[11] *Hexahapto*-C_2B_{10}. Zr-complexes;
(a) Y. Wang, H. Wang, H.-W. Li, Z. Xie, Organometallics 21 (2002) 3311;
(b) W.-C. Kwong, H.-S. Chan, Y. Tang, Z. Xie, Organometallics 23 (2004) 3098.
[12] *Hexahapto*-C_2B_{10}. Hf-complex: M.-S. Cheung, H.-S. Chan, Z. Xie, Organometallics 24 (2005) 3037.
[13] *Hexahapto*-C_2B_{10}. Co-complexes;
(a) M.R. Churchill, B.G. DeBoer, Inorg. Chem. 13 (1974) 1411;
(b) M.R. Churchill, B.G. DeBoer, J. Chem. Soc. Chem. Commun. (1972) 1326;
(c) K.J. Donaghy, P.J. Carroll, L. Sneddon, J. Organomet. Chem. 550 (1998) 77;
(d) A. Burke, R. McIntosh, D. Ellis, G.M. Rosair, A.J. Welch, Collect. Czech. Chem. Commun. 67 (2002) 991.
[14] *Heptahapto*-C_2B_{10}. Zr-complexes: M.-S. Cheung, H.-S. Chan, S. Bi, Z. Lin, Z. Xie, Organometallics 24 (2005) 4333.
[15] *Hexahapto*-PCB_8. Fe-complexes: D.E. Kadlecek, A.M. Shedlow, S.O. Kang, P.J. Carroll, L.G. Sneddon, J. Am. Chem. Soc. 125 (2003) 212.
[16] *Hexahapto*-C_3B_7. V-complexes;
(a) M.D. Wasczcak, Y. Wang, A. Garg, W.E. Geiger, S.O. Kang, P.J. Carroll, L.G. Sneddon, J. Am. Chem. Soc. 123 (2001) 2783;
(b) B.M. Ramachandran, Y. Wang, S.O. Kang, P.J. Carroll, L.G. Sneddon, Organometallics 23 (2004) 2989.
[17] *Hexahapto*-C_3B_7. Fe-complexes;
(a) C.A. Plumb, P.J. Carroll, L.G. Sneddon, Organometallics 11 (1992) 1665;
(b) C.A. Plumb, P.J. Carroll, L.G. Sneddon, Organometallics 11 (1992) 1672;
(c) M.D. Wasczcak, C.C. Lee, P.J. Carroll, L.G. Sneddon, Angew. Chem. Int. Ed. Engl. 36 (1997) 2228;
(d) B.A. Barnum, P.J. Carroll, L.G. Sneddon, Inorg. Chem. 36 (1997) 1327;
(e) B.M. Ramachandran, P.J. Carroll, L.G. Sneddon, J. Am. Chem. Soc. 122 (2000) 11033;
(f) B.M. Ramachandran, S.M. Trupia, W.E. Geiger, P.J. Carroll, L.G. Sneddon, Organometallics 21 (2002) 5078;
(g) B. Grüner, L. Mikulášek, I. Cisařová, B. Štibr, J. Organomet. Chem. 690 (2005) 2853.
[18] *Hexahapto*-C_3B_7. Ru- and Os-complexes: Ref. [17f].
[19] *Hexahapto*-C_3B_7. Co-complexes;
(a) Ref. [17b];
(b) W. Weinmann, A. Wolf, H. Pritzkow, W. Siebert, B.A. Barnum, P.J. Carroll, L.G. Sneddon, Organometallics 14 (1995) 1911.
[20] *Hexahapto*-C_3B_7. Ni-complexes: Ref. [19b].
[21] *Hexahapto*-C_3B_7. Pd- and Pt-complexes: B.A. Barnum, P.J. Carroll, L.G. Sneddon, Organometallics 15 (1996) 645.
[22] *Hexahapto*-C_3B_9. Fe-complexes: Ref. [17g].
[23] *Tetrahapto*-C_2PB_7. Co- and Ni-complexes: D. Hong, S.E. Rathmill, P.J. Carroll, L.G. Sneddon, J. Am. Chem. Soc. 125 (2003) 16058.
[24] *Hexahapto*-C_4B_7. Cr-complexes: R.B. Maynard, Z.-T. Wang, E. Sinn, R.N. Grimes, Inorg. Chem. 22 (1983) 873.
[25] *Hexahapto*-C_4B_7. Fe-complexes;
(a) W.M. Maxwell, R.F. Bryan, R.N. Grimes, J. Am. Chem. Soc. 99 (1977) 4008;
(b) Ref. [13c].
[26] *Hexahapto*-C_4B_7. Co-complexes;
(a) R.B. Maynard, E. Sinn, R.N. Grimes, Inorg. Chem. 20 (1981) 1201;
(b) Ref. [13c].
[27] *Hexahapto*-C_4B_8. Cr-complexes: Ref. [24].
[28] *Hexahapto*-C_5B_6. Fe-complexes: B.A. Barnum, P.J. Carroll, L.G. Sneddon, Organometallics 14 (1995) 4463.
[29] R.E. Williams, Chem. Rev. 92 (1992) 177.
[30] R.M. Adams, Pure Appl. Chem. 30 (1972) 681.
[31] (a) J.B. Casey, W.J. Evans, W.H. Powell, Inorg. Chem. 22 (1983) 2228;
(b) J.B. Casey, W.J. Evans, W.H. Powell, Inorg. Chem. 22 (1983) 2236.
[32] K.P. Callahan, C.E. Strouse, A.L. Sims, M.F. Hawthorne, Inorg. Chem. 13 (1974) 1393.
[33] K.A. Solontsev, L.A. Butman, I.Yu. Kuznetsov, N.T. Kuznetsov, B. Štibr, Z. Yanoushek, K. Bashe, Koord. Khim. (Russ.) 9 (1983) 993.
[34] R.V. Schultz, F. Sato, L.J. Todd, J. Organomet. Chem. 125 (1977) 115.
[35] V. Petříček, K. Malý, A. Petřina, L. Hummel, A. Línek, Acta Cryst. B35 (1979) 3044.
[36] R.R. Rietz, D.F. Dustin, M.F. Hawthorne, Inorg. Chem. 13 (1974) 1580.
[37] W. Quintana, R.L. Ernest, P.J. Carroll, L.G. Sneddon, Organometallics 7 (1988) 166.
[38] W. Quintana, Inorg. Chem. 36 (1997) 940.
[39] M.A. Benvenuto, M. Sabat, R.N. Grimes, Inorg. Chem. 31 (1992) 3904.
[40] K.W. Piepgrass, K.E. Stockman, M. Sabat, R.N. Grimes, Organometallics 11 (1992) 2404.
[41] H. Yao, M. Sabat, R.N. Grimes, P. Zanello, F. Fabrizi de Biani, Organometallics 22 (2003) 2581.
[42] J.R. Pipal, R.N. Grimes, Organometallics 12 (1993) 4459.
[43] A.R. Oki, H. Zhang, J.A. Maguire, N.S. Hosmane, H. Ro, W.E. Hatfield, M. Moscherosch, W. Kaim, Organometallics 11 (1992) 4202.
[44] A.R. Oki, H. Zhang, J.A. Maguire, N.S. Hosmane, H. Ro, W.E. Hatfield, Organometallics 10 (1991) 2996.
[45] P. Zanello, Inorganic Electrochemistry. Theory, Practice and Application, RSC, Cambridge, UK, 2003.
[46] W.E. Geiger, D.E. Brennan, Inorg. Chem. 21 (1982) 1963.
[47] A. Fessenbecker, M. Stephan, R.N. Grimes, H. Pritzkow, U. Zenneck, W. Siebert, J. Am. Chem. Soc. 113 (1991) 3061.
[48] M. Stephan, J.H. Davis, X. Meng, K.J. Chase, J. Hauss, U. Zenneck, H. Pritzkow, W. Siebert, R.N. Grimes, J. Am. Chem. Soc. 114 (1992) 5214.
[49] J.R. Pipal, R.N. Grimes, Inorg. Chem. 18 (1979) 263.
[50] (a) S. Tomlinson, C. Zheng, N.S. Hosmane, J. Yang, Y. Wang, H. Zhang, T.G. Gray, T. Demissie, J.A. Maguire, F. Baumann, A. Klein, B. Sarkar, W. Kaim, W.N. Lipscomb, Organometallics 24 (2005) 2177;
(b) H. Zhang, Y. Wang, A.K. Saxena, A.R. Oki, J.A. Maguire, N.D. Hosmane, Organometallics 12 (1993) 3933.
[51] E.J. Hauser, M.A. Curtis, M. Sabat, R.N. Grimes, J. Organomet. Chem. 536–537 (1997) 115.
[52] R. Weiss, R.F. Bryan, Acta Cryst. B33 (1977) 589.
[53] J.M. Russell, M. Sabat, R.N. Grimes, Organometallics 21 (2002) 5613.
[54] M. Stephan, J. Hauss, U. Zenneck, W. Siebert, R.N. Grimes, Inorg. Chem. 33 (1994) 4211.
[55] T.T. Chin, R.N. Grimes, W.E. Geiger, Inorg. Chem. 38 (1999) 93.
[56] J.J. Briguglio, L.G. Sneddon, Organometallics 4 (1985) 721.
[57] A.J. Borelli Jr., J.S. Plotkin, L.G. Sneddon, Inorg. Chem. 21 (1982) 1328.
[58] X. Meng, S. Waterworth, M. Sabat, R.N. Grimes, Inorg. Chem. 32 (1993) 3188.
[59] N.S. Hosmane, Y. Wang, A.R. Oki, H. Zhang, J.A. Maguire, Organometallics 15 (1996) 626.
[60] J.R. Pipal, W.M. Maxwell, R.N. Grimes, Inorg. Chem. 17 (1978) 1447.
[61] D.A. Franz, E.J. Houser, M. Sabat, R.N. Grimes, Inorg. Chem. 35 (1996) 7027.
[62] (a) W. Weinmann, F. Metzner, H. Pritzkow, W. Siebert, L. Sneddon, Chem. Ber. 129 (1996) 213;
(b) B.A. Barnum, P.J. Carroll, L.G. Sneddon, Inorg. Chem. 36 (1997) 1327.
[63] D. St. Clair, A. Zalkin, D.H. Templeton, Inorg. Chem. 11 (1972) 377.
[64] D.A. Brown, M.O. Fanning, N.J. Fitzpatrick, Inorg. Chem. 17 (1978) 1620.
[65] O. Tutusaus, F. Teixidor, R. Núñez, C. Viñas, R. Sillanpää, R. Kivekäs, J. Organomet. Chem. 657 (2002) 247, and references therein.
[66] (a) J.M. Forward, D.M.P. Mingos, T.E. Müller, D.J. Williams, Y.-K. Yan, J. Organomet. Chem. 467 (1994) 207;
(b) Y.-K. Yan, D.M.P. Mingos, D.J. Williams, M. Kurmoo, J. Chem. Soc. Dalton Trans. (1995) 3221.
[67] D. St. Clair, A. Zalkin, D.H. Templeton, Inorg. Chem. 10 (1971) 2587.
[68] A. Zalkin, D.H. Templeton, T.E. Hopkins, J. Am. Chem. Soc. 87 (1965) 3988.

[69] A.R. Kudinov, P. Zanello, R.H. Herber, manuscript in preparation.
[70] L.I. Zakharkin, V.V. Kobak, A.I. Kovredov, N.G. Fumanova, Yu.T. Struchkov, Izv. Akad. Nauk. SSSR. Ser. Khim. (Russ.) (1979) 1097.
[71] L.I. Zakharkin, V.V. Kobak, A.I. Yanovsky, Yu.T. Struchkov, J. Organomet. Chem. 228 (1982) 119.
[72] V.L. Shirokii, V.A. Knizhnikov, T.P. Konovalov, Z.P. Zubreichuk, A.A. Erdman, S.E. Nefedov, I.L. Eremenko, A.I. Yanovsky, Yu.T. Struchkov, N.A. Mayer, Izv. Akad. Nauk. SSSR. Ser. Khim. (Russ.) (1993) 764.
[73] (a) H.C. Kang, S.S. Lee, C.B. Knobler, M.F. Hawthorne, Inorg. Chem. 30 (1991) 2024;
(b) X. Yang, W.A. King, M. Sabat, T.J. Marks, Organometallics 12 (1993) 4254.
[74] (a) J.M. Forward, D.M.P. Mingos, A.V. Powell, J. Organomet. Chem. 465 (1994) 251;
(b) J.D. McKinney, F.S. McQuillan, H. Chen, T.A. Hamor, C.J. Jones, M. Slaski, G.H. Cross, C.J. Harding, J. Organomet. Chem. 547 (1997) 253.
[75] Y.-K. Yan, D.M.P. Mingos, M. Kurmoo, W.-S. Li, I.J. Scowen, M. McPartlin, A.T. Coomber, R.H. Friend, J. Chem. Soc. Dalton Trans. (1995) 2851.
[76] Y.-K. Yan, D.M.P. Mingos, T.E. Müller, D.J. Williams, M. Kurmoo, Dalton Trans. (2000) 1609.
[77] S.V. Timofeev, I.A. Lobanova, A.R. Kudinov, V.I. Meshcheryakov, O.L. Tok, P.V. Petrovskii, F.M. Dolgushin, Z.A. Starikova, V.I. Bregadze, Izv. Akad. Nauk. SSSR. Ser. Khim. (Russ.) (1979) 1097.
[78] Y.-K. Yan, D.M.P. Mingos, T.E. Müller, D.J. Williams, M. Kurmoo, J. Chem. Soc. Dalton Trans. (1994) 1735.
[79] Y.-K. Yan, D.M.P. Mingos, D.J. Williams, J. Organomet. Chem. 498 (1995) 267.
[80] J. Plešek, B. Štibr, P.A. Cooke, J.D. Kennedy, T.D. McGrath, M. Thornton-Pett, Acta Cryst. C54 (1998) 36.
[81] F.A. Gomez, S.E. Johnson, C.B. Knobler, M.F. Hawthorne, Inorg. Chem. 31 (1992) 3558.
[82] A. Varadarajan, S.E. Johnson, F.A. Gomez, S. Chakrabarti, C.B. Knobler, M.F. Hawthorne, J. Am. Chem. Soc. 114 (1992) 9003.
[83] V. Šubrtová, K. Malý, V. Petříček, A. Línek, Acta Cryst. B38 (1982) 2028.
[84] A.R. Kudinov, D.S. Perekalin, S.S. Rynin, K.A. Lissenko, G.V. Grintselev-Knyazev, P.V. Petrovskii, Angew. Chem. Int. Ed. 41 (2002) 4112.
[85] D.S. Perekalin, D.G. Golovanov, K.A. Lyssenko, P.V. Petrovskii, P. Zanello, M. Corsini, A.R. Kudinov, manuscript in preparation.
[86] G.M. Rosair, A.J. Welch, A.S. Weller, Organometallics 17 (1998) 3227.
[87] W.E. Geiger, W.L. Bowden, N. El Murr, Inorg. Chem. 18 (1979) 2358.
[88] D.E. Smith, A.J. Welch, Organometallics 5 (1986) 760.
[89] Z.G. Lewis, A.J. Welch, Acta Cryst. C48 (1992) 53.
[90] Z.G. Lewis, D. Reed, A.J. Welch, J. Chem. Soc. Dalton Trans. (1992) 731.
[91] T. Totani, H. Nakai, M. Shiro, T. Nakagawa, J. Chem. Soc. Dalton Trans. (1975) 1938.
[92] (a) J. Llop, C. Viñas, F. Teixidor, L. Victori, R. Kivekäs, R. Sillanpää, Inorg. Chem. 41 (2002) 3347;
(b) C. Viñas, J. Llop, F. Teixidor, R. Kivekäs, R. Sillanpää, Chem. Eur. J. 11 (2005) 1933.
[93] (a) A. Zalkin, T.E. Hopkins, D.H. Templeton, Inorg. Chem. 6 (1967) 1911;
(b) L. Borodinsky, E. Sinn, R.N. Grimes, Inorg. Chem. 21 (1982) 1686.
[94] R.M. Chamberlin, B.L. Scott, M.M. Melo, K.D. Abney, Inorg. Chem. 36 (1997) 809.
[95] C. Viñas, J. Pedrajas, J. Bertran, F. Teixidor, R. Kivekäs, R. Sillanpää, Inorg. Chem. 36 (1997) 2482.
[96] C. Viñas, J. Bertran, S. Gomez, F. Teixidor, J.-F. Dozol, H. Roquette, R. Kivekäs, R. Sillanpää, J. Chem. Soc. Dalton Trans. (1998) 2849.
[97] M.F. Hawthorne, C.L. Beno, D.E. Harwell, S.S. Jalisatgi, C.B. Knobler, J. Mol. Struct. 656 (2003) 239.
[98] C. Viñas, S. Gomez, J. Bertran, J. Barron, F. Texeidor, J.-F. Dozol, H. Rouquette, R. Kivekäs, R. Sillanpää, J. Organomet. Chem. 581 (1999) 188.
[99] P. Sivý, A. Preisinger, O. Baumgartner, F. Valach, B. Koreň, L. Mátel, Acta Cryst. C42 (1986) 30.
[100] I. Rojo, F. Teixidor, C. Viñas, R. Kivekäs, R. Sillanpää, Chem. Eur. J. 9 (2003) 4311.
[101] J. Plešek, S. Heřmánek, A. Franken, I. Cisarova, C. Nachtigal, Collect. Czech. Chem. Commun. 62 (1997) 47.
[102] F. Teixidor, J. Pedrajas, I. Rojo, C. Viñas, R. Kivekäs, R. Sillanpää, I. Sivaev, V. Bregadze, S. Sjöberg, Organometallics 22 (2003) 3414.
[103] J. Llop, C. Masalles, C. Viñas, F. Teixidor, R. Sillanpää, R. Kivekäs, Dalton Trans. (2003) 556.
[104] J. Plešek, B. Grüner, S. Heřmánek, J. Báča, V. Mareček, J. Jänchenová, A. Lhotský, K. Holub, P. Selucký, J. Rais, I. Cisařová, J. Čáslavský, Polyhedron 21 (2002) 975.
[105] I. Rojo, F. Teixidor, R. Kivekäs, R. Sillanpää, C. Viñas, Organometallics 22 (2003) 4642.
[106] A.N. Gashti, J.C. Huffman, A. Edwards, G. Szekeley, A.R. Siedle, J.A. Karty, J.P. Reilly, L.J. Todd, J. Organomet. Chem. 614–615 (2000) 120.
[107] (a) N. Kirillova, A.S. Zhdanov, A.I. Gusev, V.N. Kirin, S.P. Knyazev, T.V. Sokolova, Metalloorg. Khim. 2 (1989) 859;
(b) P.K. Hurlburt, R.L. Miller, K.D. Abney, T.M. Foreman, R.J. Butcher, S.A. Kinkead, Inorg. Chem. 34 (1995) 5215.
[108] P. Sivý, A. Preisinger, O. Baumgartner, F. Valach, B. Koreň, L. Mátel, Acta Cryst. C42 (1986) 28.
[109] E.C. Santos, A.B. Pinkerton, S.A. Kinkead, P.K. Hurlburt, S.A. Jasper, C.W. Sellers, J.C. Huffman, L.J. Todd, Polyhedron 19 (2000) 1777.
[110] (a) B.G. DeBoer, A. Zalkin, D.H. Templeton, Inorg. Chem. 7 (1968) 2288;
(b) P. Sivý, A. Preisinger, O. Baumgartner, F. Valach, B. Koreň, L. Mátel, Acta Cryst. C42 (1986) 24;
(c) C.-W. Tsang, J. Sun, Z. Xie, J. Organomet. Chem. 613 (2000) 99.
[111] E.M.D. Mortimer, C.B. Knobler, M.F. Hawthorne, Inorg. Chem. 35 (1996) 5750.
[112] A. Franken, J. Plešek, C. Nachtigal, Collect. Czech. Chem. Commun. 62 (2002) 746.
[113] K. Shelly, C.B. Knobler, M.F. Hawthorne, New J. Chem. 12 (1988) 317.
[114] J. Plešek, S.S. Heřmánek, Collect. Czech. Chem. Commun. 60 (1995) 1297.
[115] M.F. Hawthorne, A. Varadarajan, C.B. Knobler, S. Chakrabarti, R.J. Paxton, B.G. Beatty, F.L. Curtis, J. Am. Chem. Soc. 112 (1990) 5365.
[116] A. Petřina, V. Petříček, K. Malý, V. Šubrtova, A. Línek, L. Hummel, Z. Kristallogr. 154 (1981) 217.
[117] Y. Subrtova, V. Petříček, A. Línek, J. Ječný, Z. Kristallogr. 144 (1976) 139.
[118] J. Plešek, I. Cisařová, J. Bačkovský, Collect. Czech. Chem. Commun. 67 (2002) 569.
[119] J. Plešek, A. Franken, R. Frohlich, Collect. Czech. Chem. Commun. 62 (1997) 57.
[120] (a) M.R. Churchill, K. Gold, J.N. Francis, M.F. Hawthorne, J. Am. Chem. Soc. 91 (1969) 1222;
(b) M.R. Churchill, K. Gold, Inorg. Chem. 9 (1971) 1928.
[121] J. Vohlidal, J. Plešek, J. Sedlacek, I. Cisařová, P. Matejka, S. Hermanek, Collect. Czech. Chem. Commun. 61 (1996) 877.
[122] I. Cisařová, V. Petříček, Acta Cryst. C42 (1986) 663.
[123] F.S. McQuillan, T.A. Hamor, R. Tanna, P.R. Ashton, M.S. Tolley, C.J. Jones, J. Organomet. Chem. 549 (1997) 233.
[124] I. Cisařová, K. Malý, L. Hummel, Acta Cryst. C50 (1994) 198.
[125] (a) A. Franken, J. Plešek, J. Fusek, M. Semrau, Collect. Czech. Chem. Commun. 62 (1997) 1070;
(b) B. Grüner, I. Cisařová, A. Franken, J. Plešek, Tetrahedron: Asymmetry 9 (1998) 79.
[126] J. Plešek, B. Grüner, J. Báča, J. Fusek, I. Cisařová, J. Organomet. Chem. 649 (2002) 181.
[127] J. Plešek, B. Grüner, I. Cisařová, J. Báča, P. Selucký, J. Rais, J. Organomet. Chem. 657 (2002) 59.
[128] I. Rojo, F. Teixidor, R. Kivekäs, R. Sillanpää, C. Viñas, J. Am. Chem. Soc. 125 (2003) 14720.

[129] D.E. Harwell, J. Nabakka, C.B. Knobler, M.F. Hawthorne, Can. J. Chem. 73 (1995) 1044.
[130] J.M. Nabakka, D.E. Harwell, C.B. Knobler, M.F. Hawthorne, J. Organomet. Chem. 550 (1998) 423.
[131] C. Viñas, J. Pedrajas, F. Teixidor, R. Kivekäs, R. Sillanpää, A.J. Welch, Inorg. Chem. 36 (1997) 2988.
[132] M. Corsini, P. Zanello, A.R. Kudinov, V.I. Meshcheryakov, D.S. Perekalin, K.A. Lyssenko, J. Solid State Electrochem. 9 (2005) 750.
[133] X.L.R. Fontaine, N.N. Greenwood, J.D. Kennedy, K. Nestor, M. Thornton-Pett, S. Heřmánek, T. Jelínek, B. Štibr, J. Chem. Soc. Dalton Trans. (1990) 681.
[134] Z.G. Lewis, A.J. Welch, J. Organomet. Chem. 430 (1992) C45.
[135] U. Grädler, A.S. Weller, A.J. Welch, D. Reed, J. Chem. Soc. Dalton Trans. (1996) 335.
[136] A.R. Kudinov, D.S. Perekalin, P.V. Petrovskii, K.A. Lyssenko, G.V. Grintselev-Knyazev, Z.A. Starikova, J. Organomet. Chem. 657 (2002) 115.
[137] (a) D. St. Clair, A. Zalkin, D.H. Templeton, J. Am. Chem. Soc. 92 (1970) 1173;
(b) D.M. Schubert, D.E. Harwell, C.B. Knobler, M.F. Hawthorne, Acta. Chem. Scand. 53 (1999) 721.
[138] (a) F.V. Hansen, R.G. Hazell, C. Hyatt, G.D. Stucky, Acta Chem. Scand. 27 (1973) 1210;
(b) P.A. Chetcuti, W. Hofherr, A. Liégard, G. Rihs, G. Rist, H. Keller, D. Zech, Organometallics 14 (1995) 666.
[139] M.F. Hawthorne, J.I. Zink, J.M. Skelton, M.J. Bayer, C. Liu, E. Livshits, R. Baer, D. Neuhauser, Science 303 (2004) 1849.
[140] R.M. Wing, J. Am. Chem. Soc. 92 (1970) 1187.
[141] V. Petříček, K. Malý, A. Petřina, K. Base, A. Línek, Z. Kristallogr. 166 (1984) 1.
[142] M.R. Churchill, K. Gold, J. Am. Chem. Soc. 92 (1970) 1180.
[143] P. Zanello, A.R. Kudinov, unpublished data.
[144] R.M. Wing, J. Am. Chem. Soc. 90 (1968) 4828.
[145] R.M. Wing, J. Am. Chem. Soc. 89 (1967) 5599.
[146] H.M. Colquhoun, T.J. Greenhough, M.G.H. Wallbridge, Acta Cryst. B33 (1977) 3604.
[147] M.C. Gimeno, A. Laguna, M. Laguna, P.G. Jones, Inorg. Chim. Acta 189 (1991) 117.
[148] L.J. Todd, I.C. Paul, J.L. Little, P.S. Welcker, C.R. Peterson, J. Am. Chem. Soc. 90 (1968) 4489.
[149] (a) W. Siebert, R. Hettrich, H. Pritzkow, Angew. Chem. Int. Ed. Engl. 33 (1994) 203;
(b) R. Hettrich, M. Kaschke, H. Wadepohl, W. Weinmann, M. Stephan, H. Pritzkow, W. Siebert, I. Hyla-Kryspin, R. Gleiter, Chem. Eur. J. 2 (1996) 487.
[150] (a) J. Edwin, M.C. Böhm, N. Chester, D.M. Hoffman, R. Hoffmann, H. Pritzkow, W. Siebert, K. Stumpf, H. Wadepohl, Organometallics 2 (1983) 1666;
(b) W. Siebert, Angew. Chem. Int. Ed. Engl. 24 (1985) 943.
[151] U. Fenner, H. Pritzkow, W. Siebert, Z. Naturforsch. 49b (1994) 315.
[152] W. Siebert, M. Bochmann, J. Edwin, C. Krüger, Y.-H. Tsay, Z. Naturforsch. 33b (1978) 1410.
[153] J. Zwecker, T. Kuhlmann, H. Pritzkow, W. Siebert, U. Zenneck, Organometallics 7 (1988) 2316.
[154] J. Zwecker, H. Pritzkow, U. Zenneck, W. Siebert, Angew. Chem. Int. Ed. Engl. 25 (1986) 1099.
[155] (a) B. Štibr, J. Holub, F. Teixidor, C. Viñas, J. Chem. Soc. Chem. Commun. (1995) 795;
(b) A.M. Shedlow, P.J. Carroll, L.G. Sneddon, Organometallics 14 (1995) 4046;
(c) B. Štibr, J. Holub, F. Teixidor, C. Viñas, Collect. Czech. Chem. Commun. 60 (1995) 2023;
(d) R. Rousseau, S. Lee, E. Canadell, F. Teixidor, C. Viñas, B. Štibr, New J. Chem. 20 (1996) 277;
(e) B. Štibr, J. Holub, I. Cisařová, F. Teixidor, C. Viñas, J. Fusek, Z. Plzák, Inorg. Chem. 35 (1996) 3635;
(f) J. Holub, B. Štibr, D. Hnyk, J. Fusek, I. Cisařová, F. Teixidor, C. Viñas, Z. Plzák, P.V.R. Schleyer, J. Am. Chem. Soc. 119 (1997) 7750;
(g) B. Štibr, J. Organomet. Chem. 690 (2005) 2694.
[156] D.S. Perekalin, J. Holub, D.G. Golovanov, K. Lyssenko, P.V. Petrovskii, B. Štibr, A.R. Kudinov, Organometallics 24 (2005) 4387.
[157] J. Holub, B. Grüner, I. Cisařová, J. Fusek, Z. Plzák, F. Teixidor, C. Viñas, B. Štibr, Inorg. Chem. 38 (1999) 2775.
[158] B. Grüner, A. Lehtonen, R. Kivekäs, R. Sillanpää, J. Holub, F. Teixidor, C. Viñas, B. Štibr, Inorg. Chem. 39 (2000) 2577.
[159] B. Grüner, F. Teixidor, C. Viñas, R. Sillanpää, R. Kivekäs, B. Štibr, J. Chem. Soc. Dalton Trans. (1999) 3337.
[160] B. Grüner, J. Bačkovský, R. Sillanpää, R. Kivekäs, I. Cisařová, F. Teixidor, C. Viñas, B. Štibr, Eur. J. Inorg. Chem. (2004) 1402.
[161] J. Holub, B. Grüner, D.S. Perekalin, D.G. Golovanov, K.A. Lyssenko, P.V. Petrovskii, A.R. Kudinov, B. Štibr, Inorg. Chem. 44 (2005) 1655.
[162] B. Štibr, J. Holub, M. Bakardjiev, I. Pavlík, O.L. Tok, I. Cisařová, B. Wrackmeyer, M. Herberhold, Chem. Eur. J. 9 (2003) 2239.
[163] M. Bakardjiev, J. Holub, M.J. Carr, J.D. Kennedy, B. Štibr, Dalton Trans. (2005) 909.
[164] R.N. Grimes, E. Sinn, J.R. Pipal, Inorg. Chem. 19 (1980) 2087.
[165] J.R. Pipal, R.N. Grimes, J. Am. Chem. Soc. 100 (1978) 3083.